

POLITECNICO DI TORINO



**Politecnico
di Torino**

MASTER'S DEGREE IN ENERGY AND NUCLEAR
ENGINEERING

A.Y. 2023/2024

SEASONAL THERMAL ENERGY
STORAGE SYSTEMS IN TRONDHEIM:
POSSIBILITIES AND CHALLENGES

Advisors:

Prof. Vittorio VERDA
Prof. Elisa GUELPA

Student:

Giorgia CIAMPO

Co-Advisors:

Prof. Natasa NORD
Dr. Ali POUR AHMADIYAN

MARCH 2024

Abstract

In regions with significant heating requirements, the effective utilization of waste heat from industrial processes becomes crucial for sustainable energy practices in buildings. Norway, possessing an extensive district heating infrastructure and substantial combined heat and power generation, encounters challenges in maximizing the use of excess heat during the summer months despite its temperate climate. The constant operation of waste incineration plants, irrespective of weather conditions, necessitates thoughtful consideration for long-term heat storage solutions. Presently, a large variety of seasonal thermal energy storage technologies exist but the most convenient are the ones based on the exploitation of geothermal energy resources.

This study uses dynamic simulations performed with MATLAB software to assess the viability of integrating excess heat from waste incineration into the conventional district heating system of a newly developed residential areas.

Seasonal thermal energy storage has been modelled by using an analytical model for vertical borehole thermal energy storage.

Since this analysis is restricted to the design phase, main results concern the plot of the storage and operating fluid temperatures, the positive effect the storage has on the reduction of heat supplied by the waste incineration plant and the supply and the return temperature of the low temperature district heating.

Thus, thanks to this study this solution represents a valuable technology to store a sufficient amount of energy for district heating systems connected to waste incineration plants at high latitudes.

Contents

1	Introduction	2
1.1	Aim and Objectives	3
1.2	Limitations	4
2	State of the Art	6
2.1	Previous Works	7
2.1.1	Vilde Eikeskog: Analyses and Evaluation of the Heat Pump Based Energy Supply System Integrating Short- and Long-Term Storages .	7
2.1.2	Fredrik Schmidt: Large Scale Heat Storage for District Heating . .	8
3	Theory	10
3.1	Low Temperature District Heating Systems	10
3.2	Borehole Thermal Energy Storage	11
3.2.1	BTES Operating Principles	12
3.2.2	BHE Layout and Material	14
3.2.3	Heat Source for BHEs	15
3.3	Heat Transfer Processes in BHE	16
3.3.1	Thermal Processes Analysis	17
3.4	Local Thermal Process	18
3.4.1	Steady-flux Regime	19
3.4.2	Step-pulse Variation	19
3.4.3	Periodic Variation	20
3.5	Global Thermal Process	20
3.6	Borehole Thermal Resistance	20
4	Method	22
4.1	Analytical Methods	23
4.2	Analytical Method For A Single Borehole	24
4.2.1	G-function	24
4.2.2	G-function Procedure Development	26
4.2.3	Short-Term and Long-Term Response	31

4.2.4	Comparison of Various G-functions	32
4.3	Analytical Method for Borehole Field	33
5	System Description	37
5.1	Individual Subsystem Models	38
5.1.1	Boreholes Heat Exchanger	38
5.1.2	Heat Pump	39
5.1.3	Waste Incineration Plant	43
5.1.4	District Heating	44
5.2	Assumptions	46
6	Model Validation	47
6.1	Software Description	47
6.2	Characteristics of the Model	47
6.3	Validation of the Analytical Model	49
7	Results	52
7.1	BTES Analysis	52
7.1.1	Results for Load 1	52
7.1.2	Results For Load 2	55
7.2	Sensitivity Analysis	56
7.2.1	Sensitivity Analysis Load 1	57
7.2.2	Sensitivity Analysis Load 2	65
7.3	Long-term Storage Performances	72
7.3.1	5 Years of Only Charging	72
7.3.2	5 Years of Only Charging and 20 Years of Charging and Discharging	74
7.4	Heat Losses Evaluation	75
7.5	Effect of the HP's COP Model on the Temperatures' Profiles	77
8	Future Work	79
9	Conclusion	81
	Ringraziamenti	87

List of Figures

3.1	Single BHE configuration	12
3.2	Seasonal heat storage principle using BTES during summer (right) and winter (left) [1]	13
3.3	BHE layouts	14
3.4	U-tube BHE coupled to a GSHP	15
3.5	Borehole patterns [2]	19
3.6	Global process [3]	21
4.1	Comparison between different behaviors for the different G-functions [4] . .	32
4.2	Interactions among a 3×3 BHEs field [5]	34
4.3	Response function for 1,3 and 9 boreholes using different G-function solutions [5]	36
5.1	Overall system layout	37
5.2	Comparison between the operating mode of the BTES	38
5.3	Superimposition of step loads [6]	39
5.4	Heat pump model [7]	40
5.5	Refrigerants characteristics from BITZER manufacturer [7]	41
5.6	Compressor power and relative COP from BITZER manufacturer [7] . . .	42
5.7	HP's COP for the performance function	43
5.8	Load comparison	44
5.9	Duration curve comparison	45
6.1	G-functions behavior [5]	49
6.2	Validation from MATLAB simulation	51
7.1	Surplus and deficit for Load 1	53
7.2	Average borehole wall temperature and mean fluid temperature for Load 1	54
7.3	Surplus and deficit for Load 2	55
7.4	Average borehole wall temperature and mean fluid temperature for Load 2	56
7.5	Sensitivity to the borehole depth for Load 1	57
7.6	Sensitivity to the borehole radius for Load 1	58
7.7	Sensitivity to the number of BHEs for Load 1	59

7.8	Sensitivity to the BHEs distance for Load 1	60
7.9	Sensitivity to k_{fill} for Load 1	61
7.10	Sensitivity to k_g for Load 1	62
7.11	Sensitivity to HP's COP for Load 1	63
7.12	Sensitivity impact for Load 1	64
7.13	Sensitivity to borehole depth for Load 2	65
7.14	Sensitivity to borehole radius for Load 2	66
7.15	Sensitivity to number of BHEs for Load 2	67
7.16	Sensitivity to the distance between BHEs for Load 2	68
7.17	Sensitivity to k_{fill} for Load 2	69
7.18	Sensitivity to k_g for Load 2	70
7.19	Sensitivity to HP's COP for Load 2	71
7.20	Sensitivity impact on BTES performances for Load 2	72
7.21	5 years of only charging comparison	73
7.22	5 years of only charging and 20 years of charging and discharging comparison	74
7.23	Losses analysis on different storage parameters	76
7.24	HP's COP model impact on temperature profiles	77

List of Tables

4.1	Models for the effective borehole thermal resistance for borehole GHE [4]	27
5.1	Loads Data	45
6.1	Parameters for model validation	50

Acronyms and Abbreviations

- **BTES** - Borehole Thermal Energy Storage
- **HT-BTES** - High Temperature Borehole Thermal Energy Storage
- **BHEs** - Borehole Heat Exchangers
- **LT-DH** - Low Temperature District Heating
- **NTNU** - Norwegian University of Science and Technology
- **FLS** - Finite Line Source
- **COP** - Coefficient Of Performance
- **DHW** - Domestic Hot Water
- **ATES** - Aquifer Thermal Energy Storage
- **GWTES** - Groundwater Thermal Energy Storage
- **GHS** - Ground Heat Storage
- **HP** - Heat Pump
- **GCHP** - Ground Coupled Heat Pump
- **GHE** - Ground Heat Exchanger
- **WIP** - Waste Incineration Plant
- **BC** - Boundary Condition

Symbols

- T_f - Average Temperature of the heat carrier fluid
- T_m - Local average temperature
- T_b - Average borehole wall temperature
- R_b - Effective borehole thermal resistance
- q - Ground heat rate extracted or injected

Chapter 1

Introduction

The world is currently facing a critical juncture in its history, where the urgent need of transition to sustainable and renewable sources of energy has never been more apparent. As we tackle with the challenges of climate change, environmental degradation and the increasing energy demand for heating and cooling purposes, it has become imperative to explore and harness energy resources that have a minimal impact on the planet. In this context, geothermal energy emerges as a compelling and largely powerful solution to meet our energy needs while simultaneously addressing the pressing issues of our time.

Geothermal energy, derived from the Earth's internal heat, is recognized for its large potential as a renewable and environmentally friendly source of power. Unlike fossil fuels, geothermal energy offers a continuous and reliable energy supply that is not subject to weather conditions or to the stability of sunlight and wind. It is a baseload energy source, capable to provide a huge amount of power, making it an ideal candidate for the transition to a sustainable and low-carbon energy landscape.

Beyond a general examination of geothermal energy, the aim of this thesis is to focus on the modeling and analysis of a geothermal long-term thermal energy storage system (BTES) coupled with a low-temperature district heating network in Norway.

In this context, Norway is known for its rich geothermal resources and commitment to sustainability.

The integrated BTES and district heating system under investigation in this thesis represents a cutting-edge approach to harnessing geothermal energy. By modeling the intricate dynamics of this system, the aim is to provide valuable insights into its efficiency, sustainability, and potential for widespread adoption. Additionally, it is analyzed how this specific application of geothermal energy can play a pivotal role in Norway's energy transition, a country renowned for its commitment to renewable energy development.

In the following chapters, the aim is to deeply explore the technical aspects of geothermal thermal energy storage, the operation of low-temperature district heating networks, and the challenges and opportunities inherent in coupling these technologies. This research seeks to contribute to the understanding of how a combined BTES and district heating system can become an integral part of the global effort to reduce greenhouse gas emissions and face climate change.

At the end of the analysis, it will be more evident that geothermal energy, coupled with innovative storage solutions, play a crucial role in shaping the future of our energy landscape. The transition to such systems represents a tangible step towards a more sustainable and resilient energy future, and this thesis seeks to shed light on the path forward, with Norway serving as a beacon of inspiration in the pursuit of renewable energy excellence.

1.1 Aim and Objectives

1. Validation of the analytical method used for BTES modeling.

Claesson and Javed proposed a new method to be adopted for modeling the long-term response of a BHE. In this first stage, the algorithm implemented must return the same trend and the same value of the response function observed by Claesson and Javed.

2. Evaluation of the effective borehole thermal resistance R_b .

R_b is a crucial parameter used in BHEs modeling to quantify the amount of losses present inside each single heat exchanger.

3. Evaluation of the average borehole wall temperature T_b and average fluid temperature T_f .

Once the model for the thermal response function has been correctly validated it is possible to evaluate T_b and T_f through the *Load Aggregation Algorithm*.

4. Sensitivity Analysis development.

The borehole wall temperature and average fluid temperature inside the storage have been calculated by ranging the main storage parameters one-at-a-time and evaluating the system performance.

5. Evaluation of long-term BTES development.

Simulations are performed over an extended period of time from 5 years to 25 years analyzing different scenarios: only charging for 5 years or charging for the beginning 5 years and charging and discharging for the remaining 20 years.

6. Evaluation of thermal losses inside the storage.

The aim of this section is to estimate which of the main design parameter has a worsening effect on the system performance.

7. Evaluation of the effect of a variable COP on storage temperatures.

The goal of this section is to analyze the effect of a variable HP's COP on system performance.

1.2 Limitations

The aim of this study is to provide a valuable insights of the long-term storing technologies connected to the LT-DH network but it is important to acknowledge its limitations. Recognizing the boundaries of the methodology proposed in the following chapters is necessary for the correct understanding of the results obtained from this study.

Potential areas of improvement for these limitations are presented in Chapter 8.

Going more in depth, the most problematic aspects to discuss are related to the modeling of the BTES itself and to the model of the HP.

As far as the BTES is concerned, main restrictions are linked to the accuracy of the temperature profiles obtained from MATLAB simulations. Since data provided are monthly-based, it is possible to observe steep transitions from one month and the subsequent one instead of smoothed ones in accordance with the development of the *Load aggregation algorithm*.

To solve these problems, suitable hourly-based data should be provided and the storage simulation should be developed with more sophisticated software as TRNSYS, COMSOL or MODELICA.

Regarding the modeling of the HP, the main issue of this work is related to the steady-state treatment of the HP itself and to the BTES modeling being heat flux based more than temperature based. By using this approach it is not possible to have a real thermal coupling between the storage system and the district heating network through the HP.

To obtain an overall dynamic model of the system the HP model must be expressed as a function of the entering fluid temperatures to the heat pump [8]. This last approach represents a valid and simplified solution in absence of data from manufacturers that not always provide polynomial coefficients to build the regression model.

In conclusion, it is worth noting that the losses evaluation presented in Chapter 7 is only a rough and not precise estimation.

To obtain more meticulous results the BTES model adopted should be adapted for the

calculation of different parameters.

Chapter 2

State of the Art

The state of the art chapter serves as a comprehensive review of previous studies, research and advancements in the field of borehole seasonal thermal energy storage systems. By examining the existing literature and studies, this chapter aims to provide a deep understanding of the current knowledge, trends, and gaps in the domain. Through a systematic exploration of relevant academic publications, this chapter offers valuable insights into the evolution of system development and BTES modeling techniques highlighting key discoveries, methodologies and theoretical frameworks employed by researchers in the past.

Furthermore, this chapter critically evaluates the strengths and limitations of existing research methodologies, identifies emerging trends and areas of innovation, and discusses unresolved questions and avenues for future exploration. By synthesizing and analyzing a wide range of scholarly works, this chapter lays the groundwork for the subsequent empirical investigation and theoretical development presented in the remainder of the thesis.

Besides articles and reviews on the topic, this chapter is mainly focused on the analysis of two master theses works developed at NTNU because they accurately reflect the specific situation present in Trondheim. Moreover, the aim of that theses is to provide detailed information on how BTES should be dynamically modelled when connected to other small subsystems.

2.1 Previous Works

2.1.1 Vilde Eikeskog: Analyses and Evaluation of the Heat Pump Based Energy Supply System Integrating Short- and Long-Term Storages

In this thesis, the analysis of the entire system is carried out by considering three main units that are the long-term BTES, the short-term water storage tank and the GSHP. Firstly, they are modelled separately and then they are connected to analyze the behavior of the thermal energy system for the evaluation of the main performance parameters.

Mainly, the approach involved in this thesis is a *dynamic-state model* and only for the heat pump a *regression model* is developed.

Modeling is performed on MATLAB software.

To start with it is noticeable to highlight that in this project the system works in three different operating modes: heating mode, cooling mode and free cooling mode. In particular, being focused on the load analysis the specific operating condition between the three previously listed is decided according to the comparison between the heating and the cooling demand. Specifically, the system operates in heating mode when the heating demand is higher than the cooling demand, it operates in cooling mode when the cooling demand is larger than the heating demand while the free heating mode is realized when the heating demand is zero and the cooling demand can be fully covered by the BTES. It is worth noting that as it can be expected the system layout changes according to the operating mode.

Focusing on the BTES sub-system model, this thesis present some bottlenecks:

1. The borehole configuration is modelled considering the storage system as a control volume and applying the dynamic-state energy balance equation to it.
2. The sizing phase of the BTES has been realized by using a rule-of-thumb approach to evaluate the approximated number of borehole and the total length.
3. The size of the BTES has been carried out according to the heat pump parameters and ground properties only.
4. Mutual interactions between BHEs are not taken into consideration in this model.

Since for the BHEs a specific modeling resolution is not employed and since the sizing involves simplifications and assumptions, it is possible to derive that the results of the

temperature differences in the storage generated by the simulations are poorly realistic. Possibly, reasons of this behavior can be related to the overestimation of the size of the storage volume and to the merging effect of the fluid flow rate of each single borehole in a single large flow rate.

Thus, it can be deduced that the results obtained are generic for a thermal energy storage but not specific for BTES.

2.1.2 Fredrik Schmidt: Large Scale Heat Storage for District Heating

This work is focused on the analysis and the evaluation of the potential of HT-BTES considering not only its monthly operation but also the effects of nightboosting. In fact, as the results have shown this effect is responsible for a significant increase of the heat carrier fluid temperature and in general HT-BTES is the most suitable technology as seasonal thermal energy storage to be integrated with industrial waste heat to increase energy efficiency of heat production and to be coupled with LT-DH network to meet energy demand.

It is worth noting that in this thesis the analysis has been carried on on MATLAB for a first evaluation of the borehole thermal capacity and then, on TRNSYS as a comparative study being this software more accurate.

The storage system modeling has been performed by following different steps and making these specific assumptions:

1. Firstly, steady-state heat losses from a HT-BTES have been evaluated. Particularly, the effects of temperature levels, size and surface insulation have been analyzed to assess their impact on system performance.
2. Secondly, the shape of the storage systems is assumed to be cylindrical.
3. Then, load cycles for charging and discharging seasons on long-term and nightboosting analysis are evaluated a priori by choosing specific periods and time-slots.
4. Additionally, the storage capacity has been assumed to be equal to the amount of available excess heat during the charging period while the discharged energy yearly based is obtained as the difference between the storage capacity and the steady-state heat losses previously evaluated.
5. In order to perform a monthly based analysis, a monthly fraction is calculated for both the operating mode of the BTES according to the excess of heat production

from WIP. Once, this analysis has been carried out, the monthly injected or extracted energy is calculated as product between the fractions and the total injected or extracted energy.

6. Finally, the sensitivity analysis has been performed in order to assess the impact of top surface insulation and ground thermal conductivity on the system performance.

From this work, results have shown that the nightboosting operation is highly potential if operated during the hours of the day when the heating demand is low.

The storage capacity has a significant impact on system performance: in particular, by increasing the capacity it is possible to observe a decrease of the temperature difference between the maximum and minimum average storage temperature.

The sensitivity analysis has shown that top surface insulation and ground thermal conductivity are the two parameters that mostly affect the system performances. If on one hand, by removing the top surface insulation the annual average storage temperature declines because of the increase of the heat losses. On the other hand, low values of ground thermal conductivity decrease heat losses but increase the ground thermal resistance. Thus, it is possible to conclude that a higher temperature difference between the heat carrier fluid and ground temperature is highly desirable.

Limitations must also be included.

1. Firstly, the analyses performed on the different plants are applied to base cases and not to optimized plant. In particular, in case more specific data can be obtained from specific tests, the HT-BTES must be optimized according to specific indicators and in accordance with economic evaluations.
2. Secondly, heat pump and district heating models must be deeply analysed by using specific tools.
3. Then, even during nightboosting operating mode the heat rate extracted from the ground should be adjusted according to the demand from LT-DH network and not fixed a priori.
4. Finally, the HT-BTES requires a more specific modeling able to relate the operations of all the subsystems including the WIP, the LT-DH and the storage itself.

Chapter 3

Theory

In this section the main theoretical aspects regarding the borehole thermal energy storage and the low temperature district heating network will be presented.

3.1 Low Temperature District Heating Systems

The existing district heating systems, belonging to the second and third generation with temperatures ranging from 80 to 100°C, are encountering significant issues.

In low-energy buildings, the demand for heating at high temperature levels is diminishing. In fact, the use of high temperatures brings challenges in harnessing renewable energy sources and waste heat. Especially in areas with low heat density, the competitiveness of the DH systems is decreasing due to the higher share of distribution losses in the total heat demand. Thus, to enhance competitiveness in regions with low heat densities and low-energy buildings, minimizing heat losses is crucial for achieving high DH system efficiency [9].

In Norway, heat losses typically range from 8-15% of the delivered heat.

Low supply temperatures have the advantage of reducing the temperature difference between the pipe and the ground, thereby diminishing heat losses to the ground and potentially reducing insulation requirements in specific DH areas. LT-DH systems present better opportunities for utilizing waste heat and renewable heat sources, along with lower distribution losses. However, transitioning to LT-DH faces challenges such as high return temperatures and a low temperature difference between the supply and return temperatures in the network [9].

Especially in Northern Europe countries, several successful LT-DH projects have been

implemented.

In Lystrup, Denmark, seven low-energy buildings were connected to LT-DH to reduce distribution losses. This process involved measures like reducing pipeline dimensions, setting the supply distribution temperature to 55°C and the return one to 25°C, and using twin pipes. In addition, two substations equipped with storage tanks and high heat output heat exchangers were implemented resulting in a 75% reduction in energy use compared to traditional DH systems.

In Albertslund, Denmark, a LT-DH network was introduced for refurbished houses, achieving a 62% reduction in distribution heat losses.

In Chalvey, England, a small-scale LT-DH network supplying ten zero-emission houses demonstrated the integration of renewable energies, achieving good results in distribution loss savings, low temperature heat production, and customer satisfaction [9].

In Norway, new buildings are constructed with high standards, leading to reduced space heating demands and a decreasing demand density in the DH network. Therefore, the transition to 4th generation is preferred to diminish heat losses and optimize the utilization of renewable and waste heat sources [10].

3.2 Borehole Thermal Energy Storage

BTES belongs to the category of long-term sensible thermal energy storage systems.

Generally, sensible thermal storage acquires energy by rising or lowering the temperature of a medium with finite heat capacitance, typically water.

In long-term thermal energy storage systems, energy is stored seasonally in various media and it is exploited during periods of high heating demand and/or limited energy availability, especially in domestic applications [11].

Borehole thermal energy storage systems store thermal energy by varying the temperature of a medium, commonly water, with finite heat capacitance.

These systems utilize soil and rock as a thermal medium, making them a versatile choice for seasonal storage compared to specific formations required by alternative systems such as ATES and GWTES [12].

It is worth noting that temperature variation can impact the performance of BTES.

Limitations related to these systems include comparatively higher heat losses than insulated water tank or gravel tank systems and the drilling costs associated with the borehole field.

Regarding this last aspect, it has been noticed that drilling costs for the BHEs installation

considerably exceed that of ATES configurations [12].

To deeply understand the advantages of employing this storing technique it is important to operate a comparison between BTES and other powerful technologies.

In particular, it is worth analyzing main differences between BTES and batteries as storing technique.

If on one hand, BTES offers an attractive solution due to its reduced unit storage size and increasing energy return throughout its lifespan. On the other hand, batteries as storing technology have limited longevity due to the chemical reactions realized inside them.

Moreover, while the batteries costs ranges' are a rip-off for medium and large storage applications, BTES energy storage can lead to a substantial money saving. In this context, it is crucial to emphasize that BTES stores thermal energy and not electrical energy, resulting in significantly different capital costs [13].

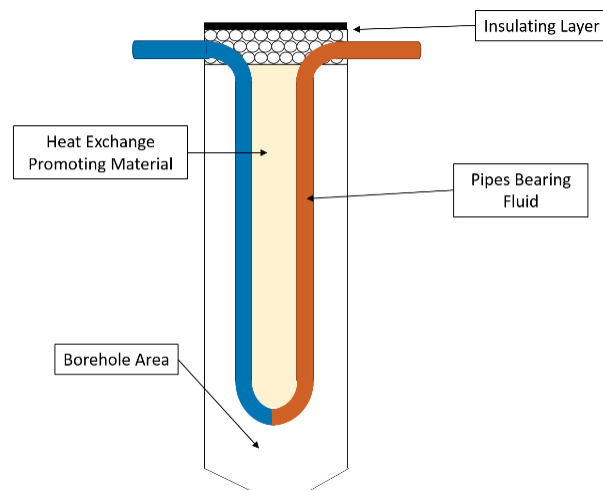


Figure 3.1: Single BHE configuration

3.2.1 BTES Operating Principles

A BTES system is a system characterized by multiple boreholes arranged in a specific pattern. Each borehole is equipped with a BHE, responsible for injecting heat into the ground during the summer and extracting heat during the winter.

The heat transfer mechanism is realized by making a heat carrier fluid circulate through the BHEs themselves [14].

Traditionally, these systems are built in a vertical borehole and filled with groundwater or other highly efficient backfilling materials [15].

The BTES design can widely vary ranging from few BHEs, for a single building, to a large

field of BHEs for an entire district.

The sizing of borehole field for domestic applications is influenced by heating and cooling loads [16].

The delivered heat can be supplied directly, or, depending on the temperature level in the BTES, it may be boosted through a HP or another auxiliary heater.

In this way, during summer the ground acts as a heat sink when the heating demand corresponds to the DHW demand, while the cooling heat rejection acts as a charging source [17].

Additionally, if the BTES temperature is sufficiently low it can also serve for cooling purposes during the summer.

During winter, BTES operation are reversed. In fact, the ground operates as an heat source. For this reason, the amount of heat extracted is used to fulfill the demand from the district heating network.

As the traditional storage systems, BTES can operate in both charging and discharging mode.

The decision is strictly influenced by the heating demand from the LT-DH network and the amount of waste heat coming from the waste incineration plant.

It is important to notice that this master thesis will specifically focus on HT-BTES systems for heating purpose while BTES operations for cooling purposes are not investigated.

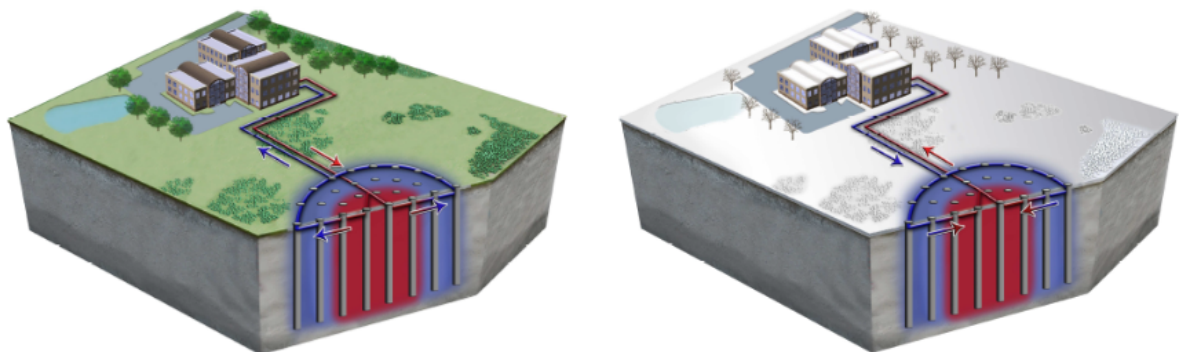


Figure 3.2: Seasonal heat storage principle using BTES during summer (right) and winter (left) [1]

3.2.2 BHE Layout and Material

The ground heat exchanger can be installed either horizontally in trenches or vertically in boreholes.

Mainly, vertical ground heat exchanger configurations are categorized by their cross-sectional geometry in U-tubes and coaxial tubes [18].

Figure 3.3 graphically shows the difference between U-tube and coaxial configuration.

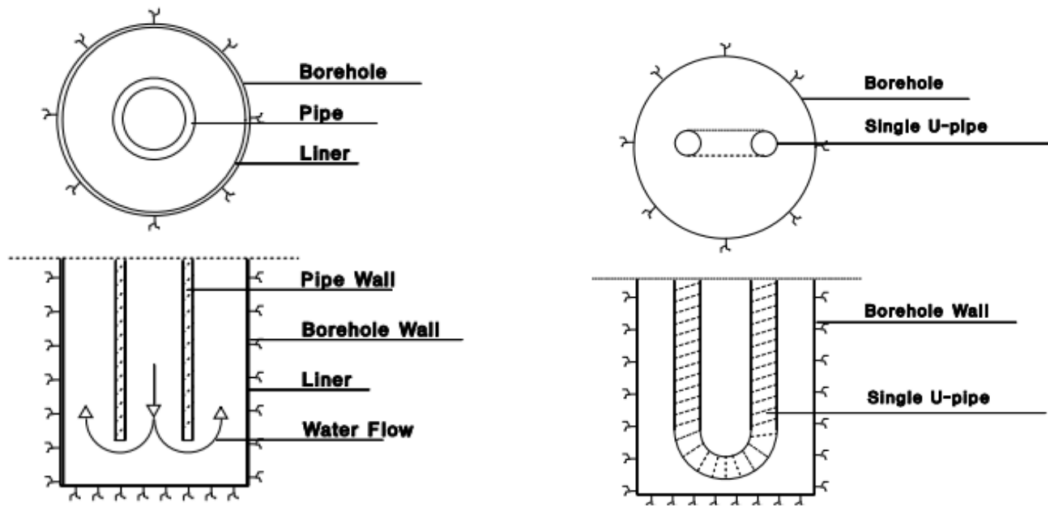


Figure 3.3: BHE layouts

Commercially, the U-tube type heat exchanges have a diameter that ranges from 1.9 cm to 5.1 cm and normally they are realized with high-density polyethylene [19].

Typically, U-tube BHEs type are integrated in a more complex system. Mostly, they are coupled to a GSHP as shown in figure 3.4.

The presence of a heat pump is necessary especially during the storage discharging season to increase the outlet storage temperature to the district heating required temperature.

The working principle of the GSHP is based on the presence of a operating fluid, typically water or a water/glycol solution, that circulates through the ground loop and the refrigerant-to-water heat exchanger to facilitate heat exchange between the ground and the refrigerant.

During the cooling season, the water carries heat away from the condenser dissipating it into the ground through the U-tube.

During the heating season, the fluid circulates through the ground loop to extract heat from the ground itself and transfer it to the evaporator [19].

Thus, one of the main advantages of a GSHP is that it can be reversed according to the

storage operating mode.

As far as the borehole field arrangement is concerned, it is important to notice that the different BHEs' layout affects the borehole thermal parameters: e.g. the borehole thermal resistance R_b and the thermal response function [19].

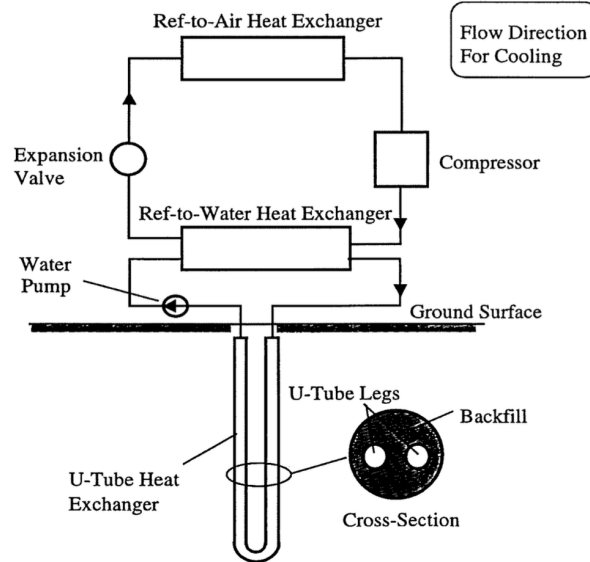


Figure 3.4: U-tube BHE coupled to a GSHP

3.2.3 Heat Source for BHEs

The potential heat sources for a BTES system are various but the selection depends on the desired temperature level to be reached inside the storage.

In the context of existing HT-BTES systems, the prevailing choices for heat sources are primarily solar thermal collectors and industrial waste heat [20].

The heat source plays a pivotal role in determining the appropriate size for the HT-BTES system. In fact, the chosen heat source can impose limitations on both the available amount of energy and the temperature level achievable in the storage.

Besides the heat source other constraints are imposed by the specific material used to fabricate the BHEs.

In this context, according to the current technologies the maximum charging temperature is assessed around 95°C [21].

A critical consideration in selecting the heat source is the existence of seasonal variations in both demand and supply. Additionally, the reliability of the HT-BTES system hinges

on the dependability of the chosen heat source for injecting energy into the system.

In this thesis, the chosen heat source is represented by the waste heat produced from a waste incineration plant.

3.3 Heat Transfer Processes in BHE

Modeling the heat transfer within a ground heat exchanger and its interaction with the surrounding soil presents complex challenges.

Beyond the structural and geometrical aspects of the heat exchanger itself, several factors influence its performance.

In this context, the main affecting elements are ground temperature distribution, soil moisture content, thermal properties of the soil, groundwater movement and potential freezing phenomena in the soil.

Thus, it becomes imperative to develop suitable tools capable of assessing and optimizing the thermal behavior of GCHP systems especially on technical perspectives [22].

To pursue these purposes, a thermal analysis should be carried out.

In particular, it is fundamental to clearly understand the heat conduction process within a single borehole between the heat carrier fluid and the borehole wall.

Then, the heat transfer between the borehole and the soil surrounding the borehole has to be analyzed, and finally, the analysis of the global process within the field with multiple boreholes is executed using the superimposition principle [1].

The previous analysis, is deeply examined in this thesis being the design phase necessary to assure the maintenance of acceptable limits for temperature rise in both the ground and the circulating fluid over the system's lifespan.

The heat transfer process in the GHE spans months or even years and, for this reason, it has a transient nature.

The heat transfer process begins with the thermal analysis of the single borehole in which conduction and convection are the prevailing heat transfer mechanisms.

The heat is then transferred towards the surrounding soil and finally, to the surrounding boreholes.

This last process is fundamental because it is responsible for an increase of the whole storage temperature.

Heat losses should also be considered and they are caused by the high temperatures inside the boreholes and the relatively low temperature of the surrounding soil.

To correctly carry out this analysis, some basic assumptions has to be done as suggested

by Hellström (1989):

- Heat transfer in the ground is only by conduction.
- Thermal properties of the ground are kept constant.

It is important to note that each heat transfer process requires a distinct modeling approach.

Typically, for the initial process the one-dimensional line-source or cylindrical-source theory is employed, taking into account that the depth of the borehole significantly exceeds its diameter. Subsequently, a long-term analysis is carried out. In this context, a two-dimensional model as the finite line-source is also employed to address axial heat flow in the ground.

Finally, the ultimate analysis aims to verify the inlet and outlet temperatures of the circulating fluid based on the borehole wall temperature and its heat flow. Typically, the heat transfer in this region is frequently simplified as a steady-state process, which has proven to be suitable for most engineering applications, barring dynamic responses within few hours [22].

This thermal analysis is crucial to estimate an important factor that is the borehole thermal resistance R_b .

Borehole thermal resistance is influenced by parameters such as the composition and flow rate of the circulating fluid, borehole diameter, the presence or absence of grouting material, U-tube material and the arrangement of flow channels.

3.3.1 Thermal Processes Analysis

As highlighted by Nordell (1994), three are the thermal processes to be considered:

1. Heat transfer between the heat carrier fluid and the borehole wall

The examination of this process involves the consideration of borehole thermal resistance.

It is important to note that the heat capacity of the materials involved is relatively limited.

Consequently, capacity effects manifest only during short-term variations. Thus, the analysis of borehole thermal resistance is conducted under steady-state conditions.

2. Heat transfer between the borehole and the surrounding ground

This is a local process and it also involves the analysis of thermal interactions between adjacent boreholes. The rate of heat transferred is established by considering the temperature difference between the heat carrier fluid and the average temperature of the surrounding ground.

This phenomenon is responsible for the rising of an additional thermal resistance within the surrounding ground which effects have to be added to the overall borehole thermal resistance.

3. Heat transfer between the borehole field and the surrounding ground

The extensive heat transfer occurring between the storage volume and the surrounding ground is known as the global process.

The primary objective of the global analysis is to compute heat losses at the storage boundary throughout a complete storage cycle.

The global process relies on the average storage temperature and does not delve into short-term temperatures' effects. This is because heat losses is contingent on fluctuations in the average storage temperature around the storage boundaries.

Following the transient thermal buildup of the HT-BTES, heat losses are attributed to both periodic temperature variations and to the annual average storage temperature. The net impact of the periodic component is assumed to be zero, allowing the calculation of annual heat loss only evaluating the annual average storage temperature.

3.4 Local Thermal Process

This process is based on the analysis of the volume of the surrounding ground around the various BHEs.

Specifically, the volume of surrounding ground around each borehole in the local thermal process depends on the borehole pattern.

Different patterns have distinct cross-sectional areas for the local ground region, indicated as A_p .

Figure 3.5 illustrates hexagonal and rectangular borehole patterns along with their respective local ground regions.

The temperature in the region A_p is the local average temperature T_m .

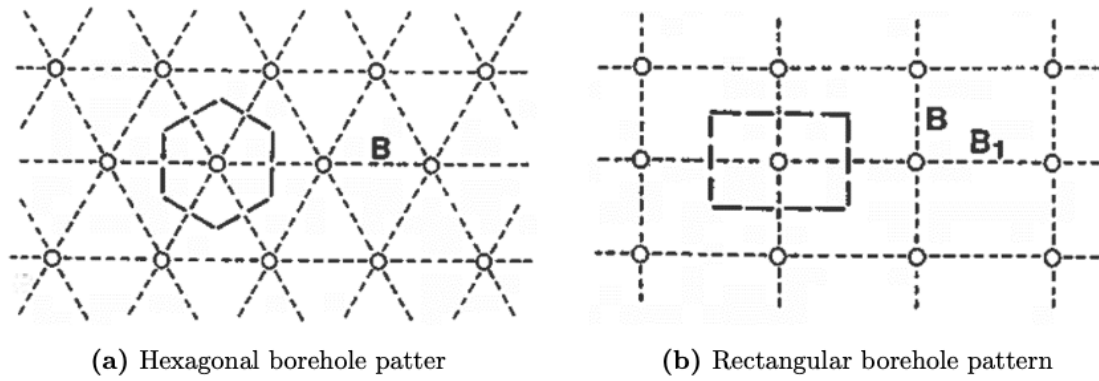


Figure 3.5: Borehole patterns [2]

As previously analyzed by Schmidt (2020), various theories can be employed to examine the local thermal process to calculate the injection rate q .

As suggested by Hellström (1991) there are three scenarios: step-pulses variation, periodic variation and steady-flux regime.

The advantage of all the preceding concepts is that it is possible to establish a relation between the rate q and the temperature difference $T_f - T_m$ [1] [2].

3.4.1 Steady-flux Regime

A steady-flux regime occurs when the injection or extraction rate remain constant for an extended duration.

In particular, the temperature difference between the heat carrier fluid and the local average temperature remains constant [2].

The symmetry of the borehole pattern and local ground region results in a zero heat flux through the outer boundary of the local ground region itself. Consequently, the temperature field's shape remains unchanged over time following an initial transient period [2].

3.4.2 Step-pulse Variation

This scenario occurs when the heat injection and extraction rate vary with time, so q is expressed as a function of time $q(t)$. The most important assumption for the step-pulse analysis is that the injection and extraction rates should be approximated by a step-wise constant value [2].

A short-term fluctuation in temperature will consequently result in a combination of step changes in the heat transfer rate, denoted as $q(t)$.

3.4.3 Periodic Variation

An alternative to the step-pulse analysis is considering that the thermal process in the BHE and local ground region comprises a steady-flux component and several superimposed periodic components [2].

The periodic component introduces the ground resistance of the local ground region, which is a complex-valued quantity.

3.5 Global Thermal Process

The global process concerns the heat transfer between the storage volume and the surrounding ground, and it comprises three distinct components that define the overall process of an HT-BTES system: the transient build-up phase, the periodic variation during an annual cycle and the steady-state component [2].

The effects of these three components are shown in figure 3.6.

The transient build-up phase is necessary to raise the temperature of the undisturbed ground from its initial value to the operating temperature. During this preheating phase, heat is only injected and not extracted. The duration of the transient thermal build-up phase can range from 3 years to 6 years, depending on the storage capacity and the annually injected energy [3].

The periodic variation results from the annual charging and discharging cycle when the HT-BTES has reached its operating temperature. These periodic variations coexist with a steady-state component as illustrated in figure 3.6.

The steady-state component is characterized by the annual average storage temperature and the annual storage heat loss is calculated based on this temperature [2].

3.6 Borehole Thermal Resistance

Each thermal process can be modelled by referring to a specific thermal resistance and it is possible to evaluate an overall thermal resistance that provides information about the global heat transfer process.

The thermal resistance within the borehole, particularly between the fluid in the U-tube heat exchanger and the borehole wall, plays a crucial role in determining the performance of a closed-loop borehole GHE.

In particular, high-efficiency systems are characterized by a low value of the borehole thermal resistance [23].

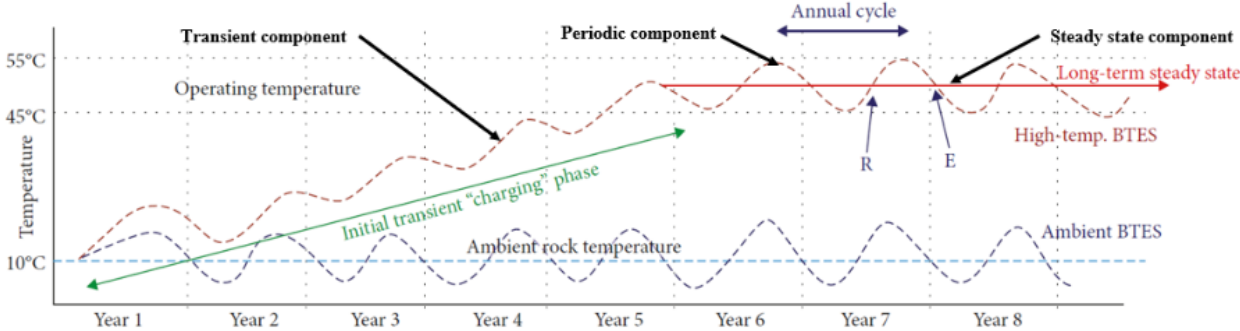


Figure 3.6: Global process [3]

Chapter 4

Method

This section performs a comparison between numerical and analytical methods used to model the single borehole and the borehole field behavior even if only analytical method is implemented in this thesis.

Analytical methods and models prove to be more advantageous than numerical methods in advancing GHE technology.

On the other hand numerical methods, including finite-difference, finite-volume and finite-element methods, offer comprehensive descriptions of the underlying physical mechanisms but they are impractical for engineering applications.

As highlighted by Li et al. (2015) main limitations related to the implementation of numerical models are:

1. Numerical methods are time consuming, especially for year-round and/or life-cycle simulations, particularly in large applications where all time and space scales are crucial and need to be addressed.
2. It is complex to develop a general grid generation program for various configurations of ground channels. This procedure is particularly challenging for in-house programming, making it difficult to create software for the analysis, design and simulation of GHS and GCHPs.
3. Most numerical models in the literature are implemented in commercial software. However, integrating commercial software into pre- and post-processing stages for system simulation in a specific application is challenging. Additionally, designers and engineers find it difficult to use computational fluid dynamics software.

As a consequence, it is preferable to adopt general design and simulation tools based on analytical heat transfer models [4].

4.1 Analytical Methods

Traditionally, borehole heat transfer research has primarily focused on assessing the long-term response of borehole heat exchangers. In this context, various analytical methods, including classical line and cylindrical source solutions proposed by Ingersoll (1954), have been derived to model the evolution of ground temperature around the borehole.

Applying these solutions to represent borehole heat transfer introduces discrepancies. These methods neglect the end effects of the heat sources and disregard the thermal properties of borehole elements. Furthermore, inaccuracies arise in determining the short-term response due to underlying assumptions about the geometry and the length of heat sources [5].

Partially the previous problem was solved by Eskilson (1987).

Eskilson (1987) addressed some of these issues by employing the finite line-source approach to develop non-dimensional thermal response solutions, known as G-functions. These G-functions, derived through numerical analysis considering transient radial-axial heat transfer in borehole heat exchangers. Moreover, they are valid for times exceeding 200 hours [24].

Eskilson also investigated thermal interactions between boreholes using a sophisticated superposition of numerical solutions for each borehole.

However, the use of G-functions for determining borehole fluid temperature has limitations and their computation is time-consuming.

Consequently, these functions are pre-computed and stored as databases in ground loop design software for various borehole heat exchanger geometries and configurations [5].

Current studies have aimed at developing analytical and semi-analytical G-functions to address flexibility concerns associated with numerically-developed G-functions.

Zeng et al. (2002) introduced an analytical G-function expression using a constant value of borehole wall temperature at the middle of the finite line-source [5] [25].

In recent years, there has been a growing interest in calculating the short-term response to optimize the design and performance of borehole heat exchangers. In this context, solution has been provided by Yavuzturk (1999) that extended Eskilson's work, developing G-functions for times ranging from 2.5 minutes to 200 hours using a numerical approach. Regarding the long-term response, the numerical and semi-analytical solutions used to determine short-term response remain computationally intensive. Javed and Claesson (2011) have recently introduced an analytical approach to determine the short-term response of borehole heat exchangers [5].

It is important to underline that analytical method is based on some fundamental assumptions as pointed out by Li et al. (2015):

1. The ground is considered either infinite or semi-infinite in extent, depending on whether the influence of the surface is taken into account [4].
2. The ground is initially characterized by a uniform temperature, referred to as the effective undisturbed ground temperature. If the surface is considered, this initial temperature can serve as a constant-temperature boundary condition (BC) for the surface [4].
3. The boundary condition for the wall of the borehole or heat transfer pipe can be either a constant flux or a constant temperature, with the constant-flux boundary condition being more convenient [4].
4. In cases where the impact of groundwater seepage cannot be neglected, the flow is typically assumed to be homogeneous and parallel to the surface. Despite the usual layered and non homogeneous nature of the ground, it is often treated as a medium with an equivalent thermal conductivity [4].

4.2 Analytical Method For A Single Borehole

4.2.1 G-function

During the first phase of the design of GHE two main interrogatives must be solved:

- Firstly, what is the heat transfer rate of a GHE over time, given a specific temperature difference between the circulating fluid and the ground [26].
- Secondly, what is the temperature difference over time considering a required heat exchange rate [26].

To start with, it is possible to provide a mathematical formulation of the entire problem considering the following equation:

$$q_l = \frac{T_f(t) - T_{s,0}}{R(t)} = \frac{\Delta T}{R(t)} \quad (4.1)$$

where T_f is the average temperature of the circulating fluid, $T_{s,0}$ is the undisturbed ground temperature, q_l is the heat transfer rate of the GHE per unit length $\frac{W}{m}$ and $R(t)$ is the total thermal resistance $\frac{mK}{W}$.

$R(t)$ in equation 4.1 is often an unknown variable that requires determination through heat transfer analysis. Despite $R(t)$ is time-dependent, analytical models commonly separate it into a time-independent component and a time-dependent component, simplifying the analysis. Therefore, one possible approach to assess existing models involves considering a time-scale context, where the constant part of R is evaluated based on specific requirements.

The transient portion of R is frequently represented as $G(t)$ and is commonly referred to as the G-function. Minor differences exist among G-functions proposed by various researchers [27][28].

The G-function was initially introduced in a dimensionless form by Ingersoll et al. (1954) and was subsequently adopted and refined by Eskilson and Claesson and Eskilson [28] [26]. The dimensionless form is widely favored for its facilitation of analysis and result summary [4].

In this context, G-functions represent thermal response factors that provide dimensionless temperature drop at the boreholes wall with a step variation for heat injection or extraction rate [29].

In contrast, the G-function used in this context holds a distinct physical interpretation: it has the dimensions of a thermal resistance and aligns entirely with the unit-step response function defined in the principle of superposition [4]

. In other terms, the unsteady thermal resistance G can be conceptualized as the temperature response in the ground resulting from a unit-step change in the heat flux, q_l [4].

Including the previous considerations, equation 4.1 can be written differently:

$$\Delta T = q_l R(t) = q_l [R_s + G(x, t)] \quad (4.2)$$

where x indicates the physical coordinate of the point under analysis and R_s is the steady component of the thermal resistance and it is a function of x .

As far as T_f is concerned, since it represents the average temperature of the ground loop for simplification it is possible to assume that it is approximately equal to the average fluid temperature.

Starting from T_f definition, the inlet $T_{f,i}(t)$ and outlet temperature $T_{f,o}(t)$ of the fluid from the BHE are derived.

The equations for $T_{f,i}(t)$ and $T_{f,o}(t)$ are the following:

$$T_{f,i}(t) = T_f(t) + \frac{q_l H}{2\rho_f c_f V_f} \quad (4.3)$$

$$T_{f,o}(t) = T_f(t) - \frac{q_l H}{2\rho_f c_f V_f} \quad (4.4)$$

where H is the BHE length, ρ_f is the density of the fluid, c_f is the specific heat of the fluid and V_f is the volumetric flow rate of the fluid.

The usage of the G-functions simplifies a lot the heat transfer model for BHE. More complex models imply energy balance equations to be coupled with computational algorithms as the finite difference method.

To sum up, some parameters must be evaluated to fully determine the thermal behavior of the borehole GHE. In fact, if on one hand the process in the borehole is assumed to be steady-state and the borehole thermal resistance R_b is the parameter adopted to model this effect. On the other hand, the process outside the borehole is time-dependent and it is modelled by the G-function [4].

4.2.2 G-function Procedure Development

To apply the G-function method the following procedure must be adopted:

1. estimation of R_b and G ;
2. calculation of T_f , $T_{f,o}$ and $T_{f,i}$.

To properly model the effective borehole thermal resistance R_b , heat transfer mechanisms should be taken into consideration.

The heat transfer within a borehole is contingent upon the arrangement of flow channels, the thermal characteristics of grouting materials and the surrounding ground. This local thermal process involves three components [2]:

1. Convective heat transfer between the circulating fluid and the inner surface of the U-shaped pipes.
2. Conductive heat transfer through the wall of the U-shaped pipe.
3. Conductive heat transfer through the backfill material.

In this context, if the time t is higher than $5t_b$, where t_b is the characteristic time associated to the borehole, the thermal process in the borehole can approach a steady-state flux. In this condition, the temperature difference between the fluid and the borehole wall remains constant.

Under these circumstances, the three previous processes can be modelled by three constant thermal resistances and their sum yields the effective fluid-to-ground thermal resistance R_b [4].

According to what is suggested by Li et al. (2015), models for R_b can be divided into empirical and theoretical.

For borehole GHE with U-shaped single pipe, the most important models can be summarised in the table 4.1:

Models	Expressions for R_b	Comments
Empirical model 1	$R_b = \frac{1}{\beta_0 k_b \left(\frac{r_b}{r_p}\right)^{\beta_1}}$	This expression uses the shape-factor concept in heat conduction. The empirical coefficients are obtained by fitting experimental data
Empirical model 2	$R_b = \frac{1}{2\pi k_b} \log\left(\frac{r_b}{\sqrt{nr_p}}\right)$	This is derived from equivalent diameter assumption. n denotes the number of pipes in a borehole
Empirical model 3	$R_b = \frac{1}{2\pi k_b} \log\left(\frac{r_b}{r_p} \sqrt{\frac{r_p}{D}}\right)$	This is for a GHE with a single U-shaped pipe. It is also derived from the equivalent-diameter assumption
Two-dimensional models	$R_b = \frac{1}{4\pi k_b} \left(\log\left(\frac{r_b^2}{2Dr_o} \left(\frac{r_b^4}{r_b^4 - D^4}\right)^\sigma - \eta\right) \right) + \frac{R_p}{2}$	The influence of k_s is represented by the dimensionless ratio r . η is equal to 0 or properly calculated being derived by the multi-pole method
Quasi-three-dimensional models	$R_b = \frac{H}{\rho_f c_f V_f} \left(\frac{T_{f,i} - T_b}{T_{f,i} - T_{f,o}} - \frac{1}{2} \right)$	$T_{f,o}$ is obtained by solving energy equations for up- and down-flow channels

Table 4.1: Models for the effective borehole thermal resistance for borehole GHE [4]

As far as empirical models are concerned, they are typically one-dimensional models, treating the U-shaped pipe as a pipe with an "equivalent" diameter. This assumption simplifies a two-dimensional geometric region into a concentric annular region, thereby transforming a complex multi-dimensional problem into a more manageable one-dimensional one [19]. As suggested by Gu et al. (1998) and by Shonder et al. (2000), possible expressions for the equivalent radius are:

$$r_{eq} = 0.414 \cdot r_o + 0.5 \cdot shank \quad (4.5)$$

$$r_{eq} = \sqrt{shank \cdot r_o} \quad (4.6)$$

$$r_{eq} = \sqrt{2} \cdot r_o \quad (4.7)$$

where r_o is the U-tube external radius and the variable shank is used to indicate the U-tube shank spacing.

Not rarely empirical models involve several empirical constants, determined by fitting experimental or computational data to the model for a specific geometric arrangement [30].

Although widely used for their simplicity, empirical models offer limited insight into the fundamental heat transfer processes, making generalization challenging.

Theoretical models, instead, can be categorized into two-dimensional and quasi-three-dimensional models. A Swedish research group proposed two two-dimensional models:

- one is derived from the steady-state line-source assumption
- the other is based on a multipole method.

The distinction between them lies in the dimensionless variables calculated through different methods.

As described by Li et al. (2015), to build-up the two-dimensional model all the boreholes' equations must be evaluated considering the two-dimensional model applied to the definition of the steady-state borehole thermal resistance.

Thus, firstly R_b is calculated according to equation 4.8:

$$R_b = \frac{1}{4\pi k_b} \left[\ln \frac{r_b^2}{2Dr_o} \left(\frac{r_b^4}{r_b^4 - D^4} \right)^\sigma - \eta \right] + \frac{R_p}{2} \quad (4.8)$$

where k_b is the thermal resistance of the backfilling material, D is half of the shank spacing between two adjacent boreholes, r_o is the external radius of the U-tube pipe, $\sigma = \frac{k_b - k_s}{k_b + k_s}$

with k_s that is the thermal conductivity of the ground and η for a single U-tube pipe is 0 and R_p is the thermal resistance of the pipe and it accounts for two heat transfer mechanism [4]:

1. convection between the circulating fluid and the inner surface of the U-shaped pipe;
2. conduction between the wall of the U-shaped pipe.

Considering the previous points, R_p is defined as:

$$R_p = \frac{1}{2\pi k_p} \ln \frac{r_o}{r_i} + \frac{1}{2\pi r_i \alpha} \quad (4.9)$$

where k_p is the thermal conductivity of the U-tube pipe, r_i is the internal radius of the U-tube pipe and α is the convective heat transfer coefficient of the fluid inside the U-tube.

The evaluation of α can be reduced to the Dittus-Boelter correlation:

$$Nu = \frac{2\alpha r_i}{k_f} = 0.023 Re^{4/5} Pr^n \quad (4.10)$$

where k_f is the thermal conductivity of the fluid inside the U-tube and n is 0.4 when the fluid is heated and 0.3 when the fluid is cooled. Moreover, the previous equation is suitable when $0.7 < Pr < 120$ and $2500 < Re < 124000$.

It is worth mentioning that even if the estimation of α is not precise R_b is not highly affected because its effects on the overall thermal resistance R_b are negligible [31].

Empirical models and two-dimensional theoretical models focus on local heat exchange at a specific depth but overlook the temperature variation in the fluid within the downward and upward channels. To address this variability, Hellstrom introduced two quasi-three-dimensional models for R_b one incorporating a uniform-flux boundary condition for the borehole wall and another employing a uniform-temperature BC [2].

Finally, it is important to observe that all the models for R_b are valid only for values of time $t > 5t_b$, indicating the achievement of a steady-flux state in the borehole. These models are commonly employed in conjunction with a G-function for the thermal process outside the borehole. Consequently, regardless of the specific G-function used, the conventional approach becomes inappropriate for $t < 5t_b$ when dealing with a rapidly fluctuating heat flux [4].

Once R_b has been evaluated it is possible to calculate the G-function.

Even in this case several models can be provided according to the accuracy that would

be reached.

In this context, different models exist: *Infinite cylindrical-surface source model*, *Infinite line-source model*, *Finite line-source model*, *Infinite moving line-source model*, *Infinite phase-change line-source model*.

It is worth noting that each model has its advantages and disadvantages and they can be applied under specific circumstances.

Mathematical expressions for the specific G-functions are presented by Li et al. (2015).

Independently on the model chosen, the ground can be treated as an infinite medium. Thus, heat transfer outside the borehole can be approximated as heat conduction in an infinite region bounded internally by the borehole wall, subject to either a constant flux or temperature boundary condition.

Carslaw and Jaeger utilized the Laplace transform method to address this, leading to the development of the infinite cylindrical-surface source model [32].

Additionally, Ingersoll et al. (1954) provided a formulation of the G-functions for buried pipe while Kavanaugh et al. (1990) used to develop the infinite cylindrical-surface source model [33] [26].

The solution provided by Carslaw and Jaeger can be mathematically expressed as:

$$T_s(t, r_b) = T_{s,0} + q_l G(t, r_b) \quad (4.11)$$

where the G-function is calculated according to what is indicated in table 4.1 or for high values of $\frac{\alpha_s t}{r_b^2}$, where α_s is the thermal conductivity of the ground, the G-function has the following expression:

$$G(r, t) = \frac{1}{4\pi k_s} \left[\ln \frac{4\alpha_s t}{r^2} - \gamma + \frac{r^2}{2\alpha_s t} \left(\ln \frac{4\alpha_s t}{r^2} - \gamma + 1 \right) \right] \quad (4.12)$$

where $\gamma = 0.5772$ is the Euler's constant.

If the radius of the borehole in a GHE is assumed to be typically small compared to its length, the borehole can be approximated to a line of infinite length.

This approach is known as the infinite line-source model.

The primary difference from the cylindrical-surface source model is the treatment of the boundary condition in correspondence of the borehole wall ($r = r_b$).

The solution to this model for the G-function is given in figure 4.1, while $T_s(t, r_b)$ can be calculated in the same way proposed by Carslaw and Jaeger.

For high values of $\frac{\alpha_s t}{r_b^2}$ the exponential integral E_1 can be approximated by:

$$\frac{1}{4\pi k_s} E_1 \left(\frac{r_b^2}{4\alpha_s t} \right) = \frac{1}{4\pi k_s} \left(\ln \frac{4\alpha_s t}{r^2} - \gamma \right) \quad (4.13)$$

Although the previous two models are widely used for their simplicity, they have limitations in terms of time scale [4].

These limitations, born from the assumptions of the specific model, make the two models be unsuitable for small periods and unable to predict GHE responses in the long-term period.

In particular, the effect of the ground surface has an impact on long-term temperature variations especially when heating and cooling loads differ from each other. When they accumulate, they can cause the average ground temperature to increase or decrease because the heat transfer to the ground surface becomes significant [4].

4.2.3 Short-Term and Long-Term Response

Short-term temperature fluctuations play a crucial role in the design, optimization and energy analysis of GCHPs [34].

The dynamic nature of heating and cooling loads in buildings, driven by factors like weather and occupancy variations and activities, results in continuous hourly variations that can be responsible of the induction of high-frequency fluctuations in ground loop temperatures [4].

According to Spitler et al. (1999) the supply and return temperatures of a ground loop can fluctuate up to 5.6 °C to 10 °C within a single day [24].

However, predicting high-frequency responses poses greater challenges than low-frequency responses due to the need to account for borehole heat capacity, involving transient heat conduction in a composite medium and considering various U-shaped tube configurations [27].

In this context, conventional analytical methods often fall short in meeting this challenge and numerical methods are commonly employed to address high-frequency responses [4].

Another approach to model the short-term response of a GHE involves simplifying the geometrical arrangement in the borehole [35].

Many short-term analytical models adopt the equivalent-diameter assumption, which transforms a complex geometry problem into one involving a relatively simple hollow cylindrical composite region [4].

An alternative method for modeling the short-term response of a GHE is based on Jaeger's instantaneous line-source solution for a cylindrical composite medium. This method addresses challenges related not only to composite media but also to the geometric configuration of heat exchange channels, encompassing single and double U-shaped tubes, W-shaped channels and helical coils [27] [36].

Despite its complexity, this model, belonging to the group of infinite line-source models, provides a valuable tool for short-term predictions, being suitable for different geometrical configurations [4].

However, this approach is not appropriate for predicting long-term thermal processes in cases where there is an unbalance between heat injection and extraction in the GHE [4].

4.2.4 Comparison of Various G-functions

According to the analysis carried out by Li et al. (2015), it is possible to operate a comparison between six analytical G-functions employed to compute the temperature response to a unit-step heat transfer rate ($q_l = 1 \frac{W}{m}$) for a single U-tube borehole GHE.

These functions include the infinite cylindrical-surface source model (equation 4.11), the infinite line-source model (equation 4.11), the simplified infinite line-source model (equation 4.7), two finite line-source models and the composite-medium line-source model.

Graphically, comparisons between different G-functions are summarized in figure 4.1:

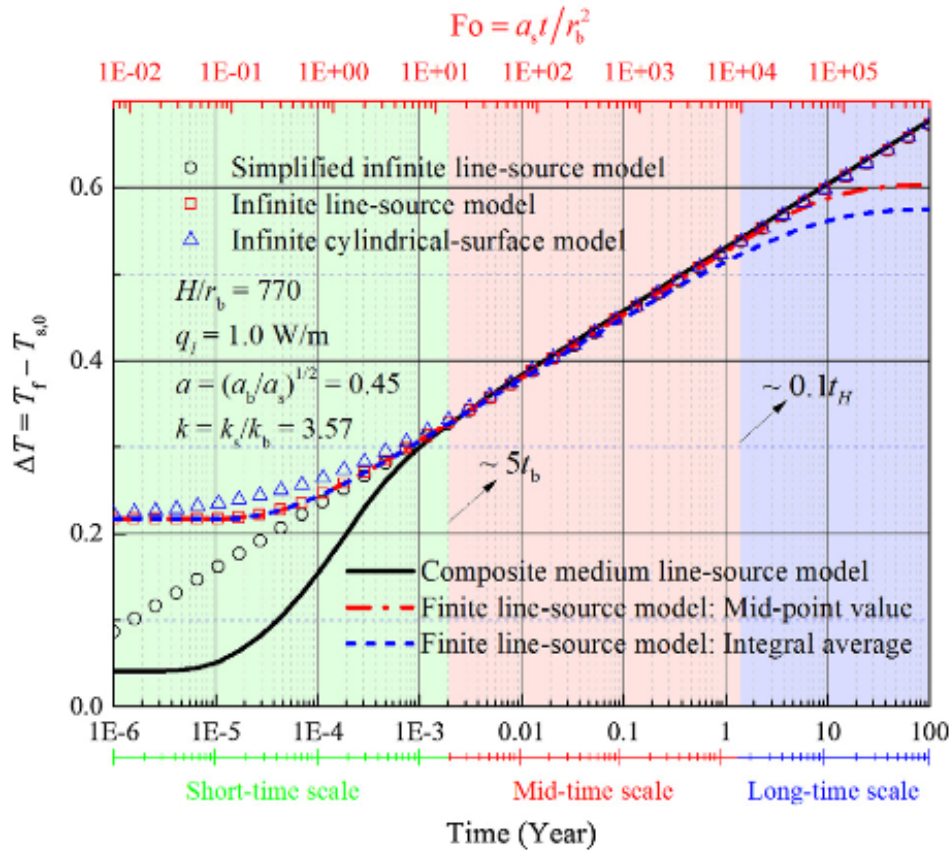


Figure 4.1: Comparison between different behaviors for the different G-functions [4]

Figure 4.1 illustrates the calculated temperature responses and the input parameters. The time range extends up to 100 years and is divided into three sub-intervals: short-time scale, medium-time scale and long-time scale. Thermal responses are reasonably consistent in the medium range, covering several hours to one year [4]. In the long-term response, all models assuming an infinitely long borehole yield are characterized by temperature responses that increase to infinity, while the finite line-source models show temperatures approaching a steady state. This suggests that the use of an infinitely long model results in an overestimation of temperature variation, leading to a more conservative borehole GHE design, despite the unavailability of long-term experimental data [4].

It is worth emphasising that figure 4.1 highlights a significant difference in the calculated short-term responses. Conventional models using steady-state thermal resistance, as infinite cylindrical-surface model, conventional infinite and finite line-source models, produce temperatures noticeably higher than those predicted by the composite-medium line-source model. This difference arises due to the neglect of the heat capacity of the grouting material in the borehole [4].

In conclusion, all examined models can be used to predict medium-term temperature responses. The composite-medium line-source model or similar models addressing borehole heat capacity should be employed for short-term responses, while the finite line-source models are suitable for long-term predictions [37].

However, these models, designed for a single-borehole GHE, cannot handle thermal interactions among GHEs [4].

For these reasons, for a more detailed system's design BTES model should match the finite-line source and the interactions among BHEs in the same model.

4.3 Analytical Method for Borehole Field

To handle the thermal interactions among the BHEs field, Claesson and Javed (2011) proposed a new method starting from the Laplace transformations and aimed to model the long-term response.

In this context, the long-term step response is derived from a continuous line heat source with a strength of $q_0 \left(\frac{W}{m}\right)$ along the borehole at $x = 0, y = 0$, and $D < z < D + H$, where D is the buried depth and H is the borehole length.

The initial ground temperature is zero and the heat emission begins at $t = 0$. The solution is obtained by integrating a point heat source along the borehole from 0 to t [5].

This approach can be adopted to model both the thermal response of the single borehole and the thermal response of the entire field.

For the single borehole the mathematical formulation of the problem is the following:

$$\bar{T}_{ls}(r, t) = \frac{q_0}{4\pi\lambda} \cdot \int_{1/\sqrt{4at}}^{\infty} ds \cdot e^{-r^2s^2} \cdot \frac{I_{ls}(Hs, Ds)}{H \cdot s^2} \quad (4.14)$$

where

$$\begin{aligned} I_{ls}(h, d) &= 2 \cdot ierf(h) + 2 \cdot ierf(h + 2d) - ierf(2h + 2d) - ierf(2d) \\ ierf(X) &= \int_0^X erf(u)du = X \cdot erf(x) - \frac{1}{\sqrt{\pi}}(1 - e^{-X^2}) \\ erf(X) &= \frac{2}{\sqrt{\pi}} \int_0^X e^{-v^2} dv \\ h &= H \cdot s \\ d &= D \cdot s \end{aligned} \quad (4.15)$$

For the entire field, the interactions among the different boreholes must be taken into consideration.

Considering a 3×3 borehole GHEs configuration, where B is the distance between two adjacent boreholes, the new method proposed takes into consideration the mutual distance between the heat exchangers in each direction as highlighted in figure 4.2.

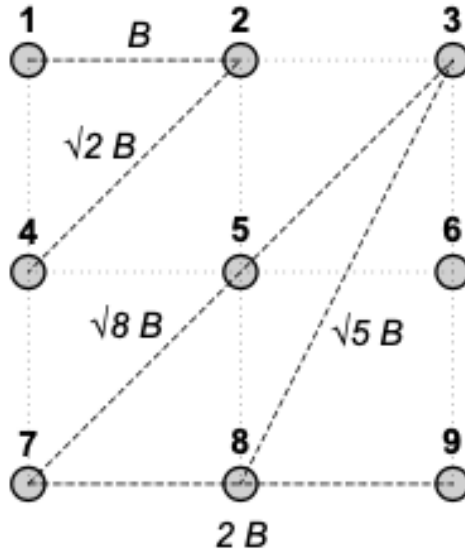


Figure 4.2: Interactions among a 3×3 BHEs field [5]

In this case, the equations used to model the interactions between N borehole GHEs start from the evaluation of the mean temperature along the borehole wall for any borehole i [5]:

$$\bar{T}_{bw,i}(t) = \sum_{j=1}^N \bar{T}_{ls}(r_{i,j}, t) \quad (4.16)$$

where $r_{i,j}$ is used to denote the mutual radial distance between the borehole i and j . In particular, this distance should be adjusted considering that:

$$r_{i,j} = \begin{cases} r_b & \text{when } i = j \\ \sqrt{(x_i - x_j)^2 + (y_i - y_j)^2} & \text{when } i \neq j \end{cases} \quad (4.17)$$

Considering that [5]:

$$\frac{1}{N} \sum_{i=1}^N \bar{T}_{bw,i}(t) = \frac{1}{N} \sum_{i=1}^N \sum_{j=1}^N \bar{T}_{ls}(r_{i,j}, t) \quad (4.18)$$

Using the equation 4.14, the mean borehole wall temperature can be written in the following way [5]:

$$T_N(r, t) = \frac{q_0}{4\pi\lambda} \cdot \int_{1/\sqrt{4at}}^{\infty} ds \cdot I_e(s) \cdot \frac{I_{ls}(Hs, Ds)}{H \cdot s^2} \quad (4.19)$$

where $I_e(s)$ can be written as [5]:

$$I_e(s) = \frac{1}{N} \sum_{i=1}^N \sum_{j=1}^N (e^{-r_{i,j}^2 s^2}) \quad (4.20)$$

As highlighted by Javed and Claesson (2011) in their study, comparing long-term and short-term fluid temperatures predicted by the new method with those from Eskilson's G-functions for different borehole GHEs configuration it is possible to deduce that:

- For a single borehole and three boreholes in a straight line, the long-term fluid temperatures align closely between the new method and Eskilson's g-functions up to 25 years [5].
- For nine boreholes in a square, the agreement is robust up to 10 years and reasonably good thereafter [5].

These results are shown in figure 4.3:

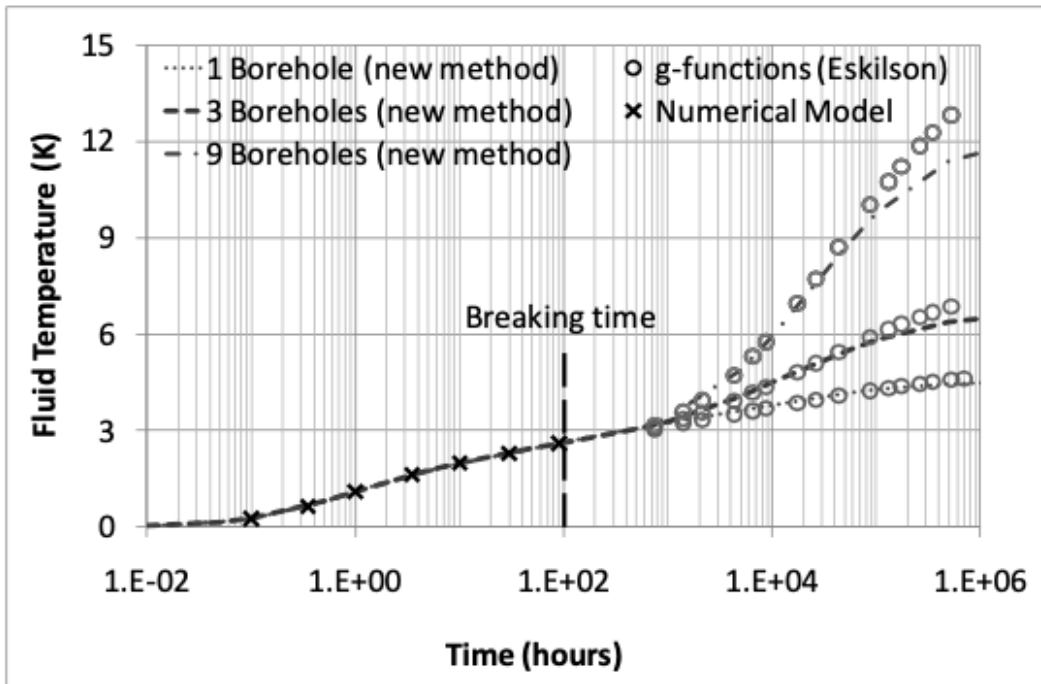


Figure 4.3: Response function for 1,3 and 9 boreholes using different G-function solutions [5]

Discrepancies between fluid temperatures predicted by the new method and Eskilson's G-functions escalate with time and the number of boreholes but remain relatively modest within the first 25 years. Moreover, the short-term fluid temperature predicted by the new model concurs with the numerical solution [5].

For a single borehole a closed-form formula has been established to determine the long-term step response, while multiple boreholes utilize a systematic approach to calculate the long-term response. The predicted long-term response from the new method aligns well with Eskilson's G-functions [5].

Furthermore, it is important to underline that the previous approach is suitable for the calculation of the borehole wall temperature for any values of heat injection and extraction rate $q_0 \left(\frac{W}{m} \right)$ considering a step response function [5].

Chapter 5

System Description

The system under analysis is a long-term seasonal thermal energy storage thought to operate in two different operating modes: charging during summer season and discharging during winter season coupled to a waste incineration plant and to a LT-DH. The entire system has the following layout:

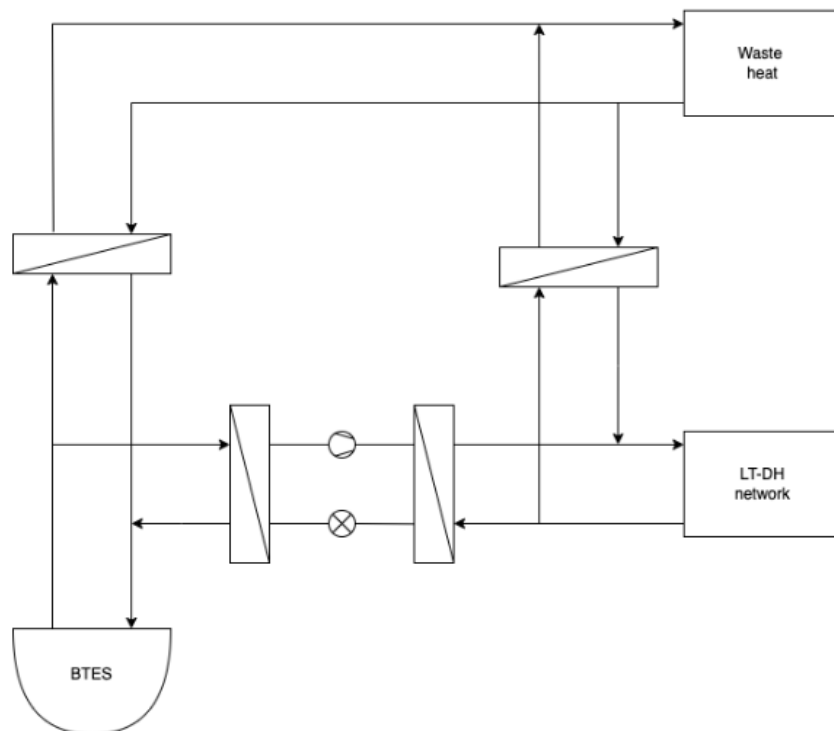


Figure 5.1: Overall system layout

From the above figure it is possible to deduce that the main system can be decomposed in

three main subsystems: the BTES, the LT-DH system and the waste incineration plant. The system layout is modified according to the different operating modes of the storage system in this way:

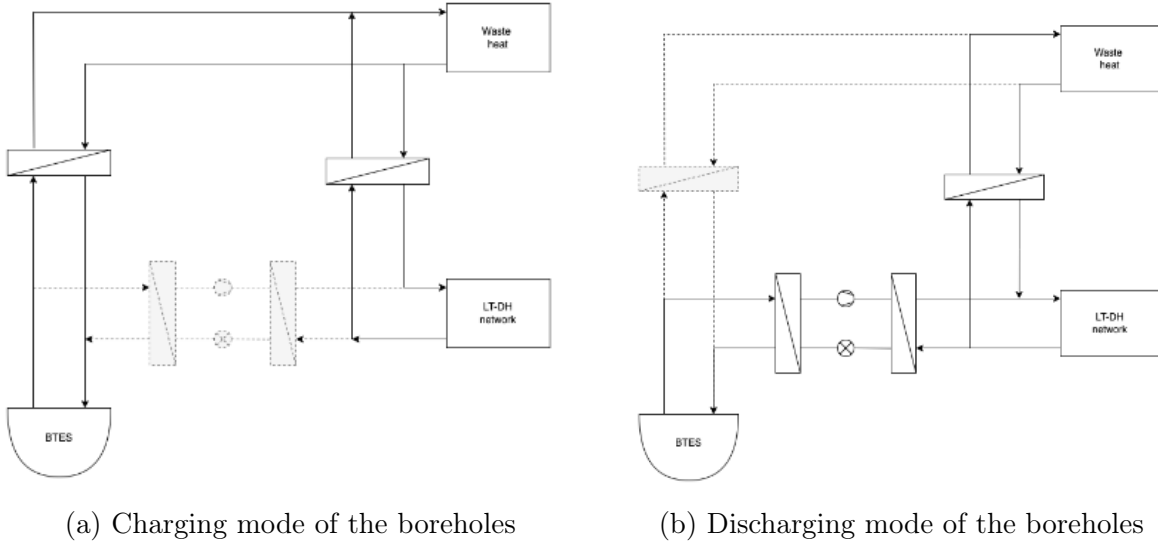


Figure 5.2: Comparison between the operating mode of the BTES

5.1 Individual Subsystem Models

5.1.1 Boreholes Heat Exchanger

The method employed in the analysis of the BHEs for the calculation of the amount of energy injected in and extracted from the ground is the ASHRAE Tp8 method and the algorithm to implement is the so called *Load Aggregation Algorithm*.

Basically, the equation used to model the BHEs aims to evaluate the borehole wall temperature by using the G-function in the finite-line source model.

In this context, the mathematical formulation of the problem is:

$$T_b - T_0 = \frac{q}{2 \cdot \pi \cdot \lambda_s} \cdot g \left(\frac{t}{t_s}, \frac{r_b}{H}, \frac{B}{H}, \text{boreholefield} \right) \quad (5.1)$$

According to the ASHRAE Tp8 method, the value of the heat flux q used in equation 5.1 is calculated by means of accumulating step changes in heat transfer rates such that the borehole wall temperature can be computed by overlaying the distinct responses at each time step [6].

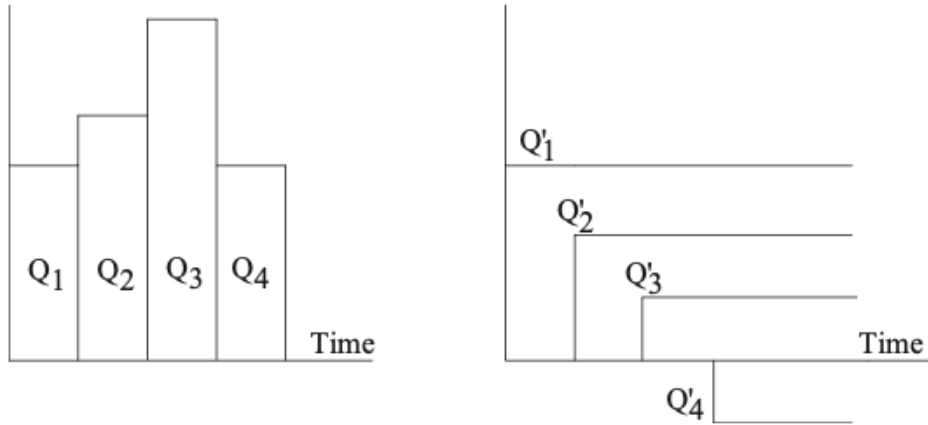


Figure 5.3: Superimposition of step loads [6]

For a given configuration of BHEs, the thermal response of the ground to a load that varies with time can be evaluated by breaking down the load into pulses and employing temporal superposition.

Figure 5.4 illustrates the process of combining responses over four months of heat rejection. As it is visible from the above figure, the fundamental heat pulse ranging from zero to Q_1 is applied throughout the entire four-month duration and is effective as $Q'_1 = Q_1$. Subsequent pulses are then superimposed, with $Q'_2 = Q_2 - Q_1$ effective for three months, $Q'_3 = Q_3 - Q_2$ effective for two months, and finally, $Q'_4 = Q_4 - Q_3$ effective for one month. Consequently, the dynamic borehole wall temperature can be determined by accumulating the ground thermal responses to these four sequential pulses [6]. Thus, according to these considerations the final equation is:

$$T_b = T_0 + \sum_{i=1}^n \frac{q_i - q_{i-1}}{2 \cdot \pi \cdot \lambda_s} \cdot g \left(\frac{t_n - t_{i-1}}{t_s}, \frac{r_b}{H} \right) \quad (5.2)$$

In the specific case of this thesis, the heat pulses have been calculated by evaluating the surplus defined as difference between heat rate from the waste incineration plant and the heating demand from the district heating network for the entire year.

5.1.2 Heat Pump

The heat pump is characterized by four components: evaporator coupled to the ground, compressor, condenser coupled to the DH network and expansion valve. The model adopted in this thesis is a regression model built by using compressor data from manufacturer BITZER.

It is worth noting that only for the HP a steady-state model is adopted to carry out the majority of the analysis.

To provide a different scenario, a semi-dynamic model of the heat pump is also included. In both cases, the heat pump can be graphically schematized in the following way:

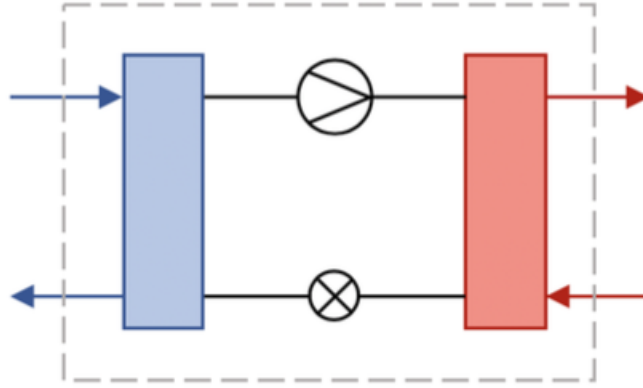


Figure 5.4: Heat pump model [7]

5.1.2.1 Regression Model

To realize a proper setup of this model the return temperatures from the evaporator T_o and the compressor T_d has been taken constant.

In the BITZER software there is a variety of compressor types and operating conditions from which users can choose.

Using the input variables T_o and T_d the software is able to generate polynomials for compressor power, evaporator capacity, condenser capacity and condenser temperature. These polynomials are computed across various operational scenarios to produce extensive data and finally, a curve fitting regression is executed to derive functions for condenser, compressor, evaporator capacities, and condenser temperature.

The coefficients for these polynomials are then incorporated into the MATLAB model [7]. Equations with polynomials used in the model are:

1. Evaporator capacity function:

$$Q_{cl,0} = q_1 + q_2T_o + q_3T_o^2 + q_4T_o^3 + q_5T_d^3 + q_6T_d + q_7T_dT_o + q_8T_dT_o^2 \quad (5.3)$$

2. Condenser capacity function:

$$Q_{cd,0} = C_1 + C_2T_d + C_3T_o + C_4Q_{cl,0} + C_5T_dT_o + C_6T_dQ_{cl,0} + C_7T_o^2 + C_8Q_{cl,0}T_o \quad (5.4)$$

3. Compressor power function

$$P_{com,0} = P_1 + P_2T_o + P_3T_d + P_4Q_{cl,0}T_d + P_5T_o^2 + P_6T_dQ_{cl,0}^2 + P_7Q_{cl,0} + P_8Q_{cl,0}^2T_o \quad (5.5)$$

4. Condenser temperature function

$$T_c = a_1T_d + a_2T_o + a_3T_o^2 + a_4 + a_5T_oT_d + a_6T_o^3 + a_7T_d^2 + a_8T_dT_o^2 \quad (5.6)$$

Once the compressor power function has been evaluated, the proper compressor must be chosen.

In the software database there is a bunch of 15 compressors characterized by different refrigerants and temperature levels T_o and T_d .

In this work, the most suitable compressor has been chosen according to the heating demand from DH. In particular, the compressor power has to be comparable to or slightly higher than the demand to be sure to fulfill the DH network's requirements.

The following figures contain information on the refrigerant properties and the compressor capacities.

The compressor chosen to develop this thesis is the model OSKA95103-K with a nominal capacity in heating mode of approximately 1.4 MW.

Index	Model	Series	Type	Refrig*	To[°C]	Tc[°C]
1	8FE-70Y	Semi-Hermetic	Reciprocating	R134a	-20/11	20/80
2	HSK8591-180	Semi-Hermetic	Screw	R134a	-20/20	20/70
3	CSH951113-320Y	Compact - CSH	Screw	R134a	-45/20	10/60
4	OSK8591-K	Open - OSK(A)	Screw	R134a	-20/20	20/70
5	W6FA-K	Open type	Reciprocating	R717	7/15	10/55
6	OSKA95103-K	Open - OSK(A)	Screw	R717	-20/12	20/65
7	OSHA7452-K	Open - OSHA	Screw	R717	-5/25	18/60
8	OSHA7472-K	Open - OSHA	Screw	R717	-5/25	18/60
9	GSD80485VA	-	Scroll	R410A	8/20	20/65
10	8FE-70Y	Semi-Hermetic	Reciprocating	R404A	-20/7	10/55
11	6F2Y-K	Open Type	Reciprocating	R404A	-45/8	20/55
12	HSK8591-180	Semi-Hermetic	Screw	R404A	-20/7	10/55
13	OSK8591-K	Open - OSK(A)	Screw	R404A	-20/7	10/55
14	4NSL-30K	Semi-Hermetic	Reciprocating	R744	-50/-15	-20/15
15	6CTE-50K	Semi-Hermetic	Reciprocating	R744	-20/0	5/30

Figure 5.5: Refrigerants characteristics from BITZER manufacturer [7]

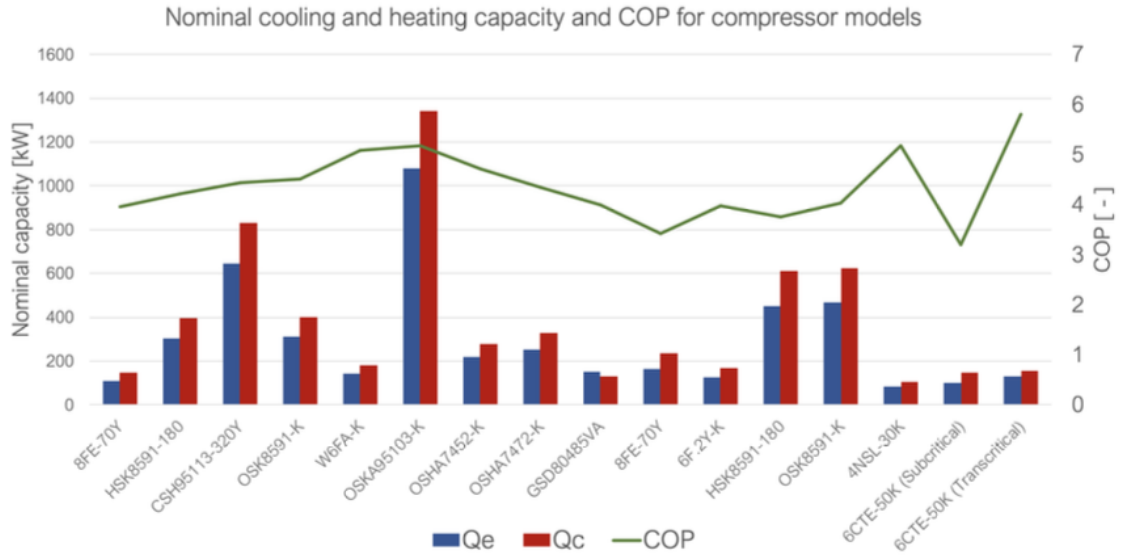


Figure 5.6: Compressor power and relative COP from BITZER manufacturer [7]

5.1.2.2 Performance Function

The use of a performance function is involved in order to estimate the effect of a variable COP on the system performance.

In fact, the regression model introduces a strong limitation due to the fact that the HP's COP is constant and its value is assessed to a minimum acceptable value for these applications.

Going more in depth with this approach, the expression chosen for the COP is a function of the nominal COP and of the temperature difference between the outdoor temperature and the nominal temperature that is the temperature provided by the manufacturer at which the COP assumes its nominal value.

$$COP = COP_{nom} \cdot (1 + 0.024 \cdot \Delta T) \quad (5.7)$$

According to this procedure, results from MATLAB simulations shown in figure 5.7 are in accordance with the theory. In fact, COP increases as the outdoor temperature increases while it decreases as the outdoor temperature decreases.

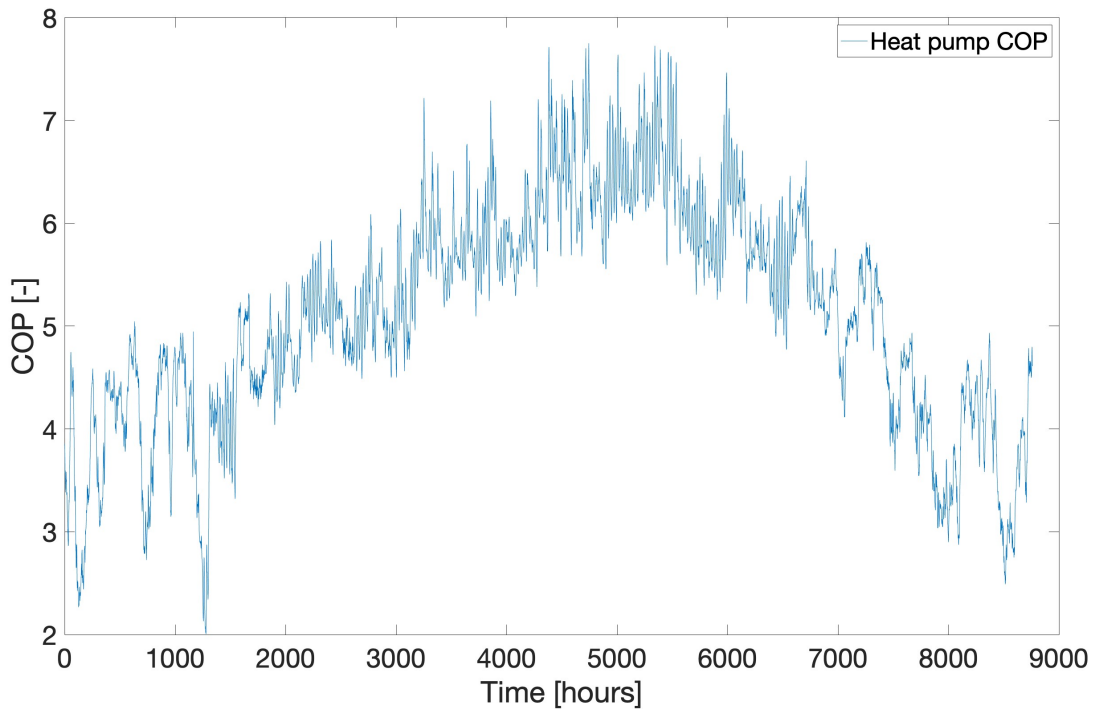


Figure 5.7: HP's COP for the performance function

5.1.3 Waste Incineration Plant

Data and information about waste-to-energy in Norway have been taken from the previous study of Schmidt (2020) in his master thesis.

According to the feasibility study performed by Schmidt it has been possible to deduce that the main reason why in Norway waste incineration is a prominent heat source in the DH sector is because it yields high amount of thermal energy.

The combination of waste incineration as a waste handling method and a heat source in the district heating sector generates substantial amount of excess heat due to the relatively constant supply and incineration of waste and the significant seasonal fluctuations experienced by the heating demand in the DH network [1].

Moreover, in his study Schmidt emphasizes that main advantages of using HT-BTES as a long term TES for excess heat from waste-to-energy DH sector in Norway offers several advantages [1]:

- Enhanced energy efficiency at district heating plants.
- Reduction of peak loads through seasonal storage.

- Establishment of a low-emission thermal energy station.

Furthermore, it is worth noting that the quantity of available excess heat varies significantly based on the capacity and size of the district heating plant [1].

5.1.4 District Heating

Data about the heating loads are representative of Norwegian district and they are taken from Eikeskog thesis presented in [7].

In this context, two different kind of loads are analysed. Data are provided on hourly base and as it is visible from figure 5.8 Load 1 is characterized by less seasonal variations in the heating demand while Load 2 has large seasonal differences in the demand [7].

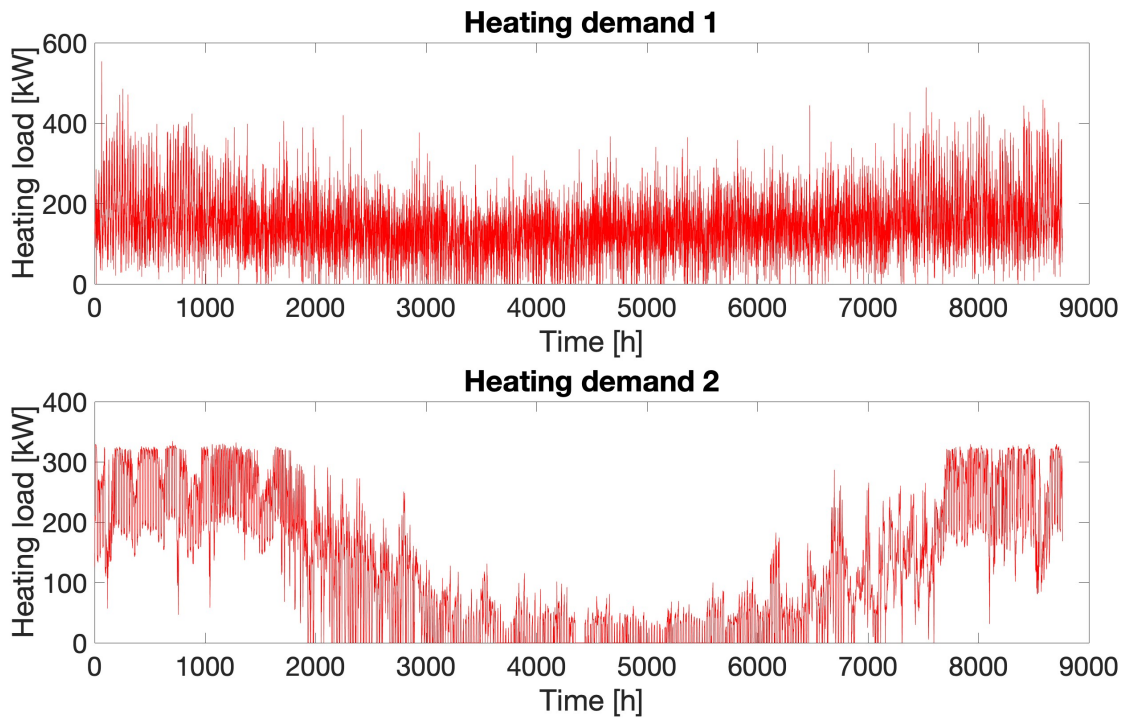


Figure 5.8: Load comparison

To evaluate the maximum value of the heating demand the duration curve is provided for both the Load 1 and Load 2.

The duration curve is extremely useful during the design phase of a DH network because it is able to provide an estimation of the peak power required from the network even for

a reduced amount of time.

From the duration curve it is also possible to calculate the base power that has to be provided with very big and expensive plants that should operate for an higher amount of equivalent hours to be economically sustainable.

The remaining time, peaks should be satisfied by other devices as boilers.

The duration curve for both the loads is:

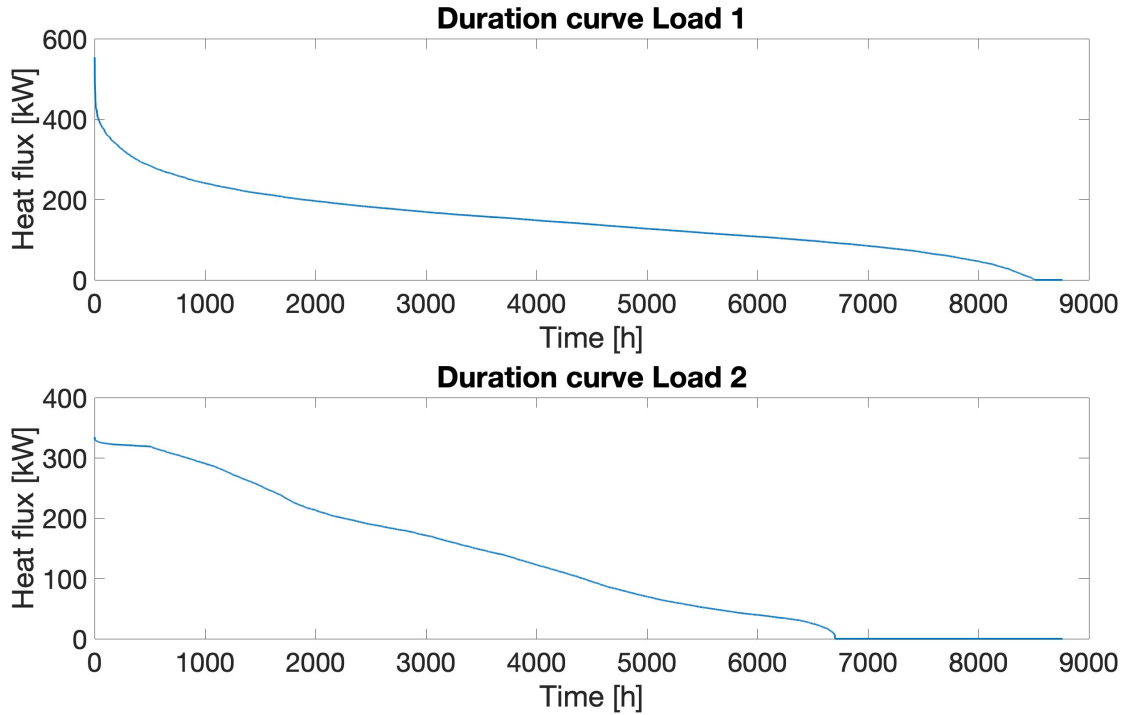


Figure 5.9: Duration curve comparison

From figure 5.9, it is possible to deduce that:

Load	Q_{\max}
1	553.6 kW
2	334.7 kW

Table 5.1: Loads Data

5.2 Assumptions

Assumptions are significant to carry out the model. The most important ones are presented in the following section:

1. *Ground properties.* Ground properties are assumed considering typical or average values in Norway. However, accurate analysis to determine the specific properties for the actual location are necessary.
2. *Load treatment.* Only heating loads for a building or area are analyzed and combined in a single load, without distinguishing between domestic hot water and space heating.
3. *Borehole wall temperature.* The borehole wall temperature T_b evaluated by the model corresponds to the temperature gradient observed in the ground after the charging and discharging processes.
4. *Conductive heat transfer mechanism.* In the ground the main heat transfer mechanism is by conduction.
5. *Ideal heat transfer mechanism in the overall system.* Losses in the system are null, such that the energy injected is assumed to be equal to the energy from the WIP while the energy withdrawn is equal to the load from LT-DH.

Chapter 6

Model Validation

The aim of this section is to compare the thermal response function obtained from the model implementation in MATLAB with the results presented by Cimmino et al. (2014). As a matter of fact, thermal response factors are widely used to predict the performance of the BHEs field.

6.1 Software Description

The BTES model has been implemented in MATLAB.

MATLAB, short for "Matrix Laboratory," is a powerful mathematical software tool widely employed for numerical computations, simulations, and data visualization.

Its power resides in its exceptional performance capabilities and an intuitive user-friendly environment that utilizes familiar mathematical notations.

One of the primary advantages of MATLAB is its efficiency in handling problems involving matrix and vector operations.

Additionally, MATLAB provides a high level of flexibility and transparency, making it a preferred choice for various scientific applications [1] [7].

6.2 Characteristics of the Model

Analytical solutions to the transient heat transfer in the ground, such as the FLS method, offer the possibility of generating thermal response factors.

In this context, as highlighted by Cimmino et al. (2014) three distinct BCs for the derivation of G-functions using the FLS method have been applied each serving a specific

purpose [29].

BC-I: Uniform Heat Extraction Rate

- Heat is uniformly extracted along the entire boreholes' length.
- Equal heat extraction rates are maintained across all boreholes.
- Average temperatures along the boreholes' length may vary.

BC-II: Uniform Heat Extraction Rate with Equal Average Temperature

- Heat is uniformly extracted along the boreholes.
- Average temperatures along the boreholes' length are maintained equal for all boreholes.

BC-III: Uniform Borehole Wall Temperature

- Borehole wall temperature is kept uniform along the boreholes' length.
- Uniform borehole wall temperature is maintained across all the BHEs.

While generating G-functions with BC-I is straightforward due to the known heat extraction rate, BC-II and BC-III present challenges as both heat extraction rates and borehole wall temperatures are unknown.

Simulations conducted on BC-II has shown an improvement of the G-function estimation, addressing some issues observed with BC-I, especially in larger bore fields with closely packed boreholes.

However some discrepancies with Eskilson's G-functions can be observed when using BC-III [29].

6.3 Validation of the Analytical Model

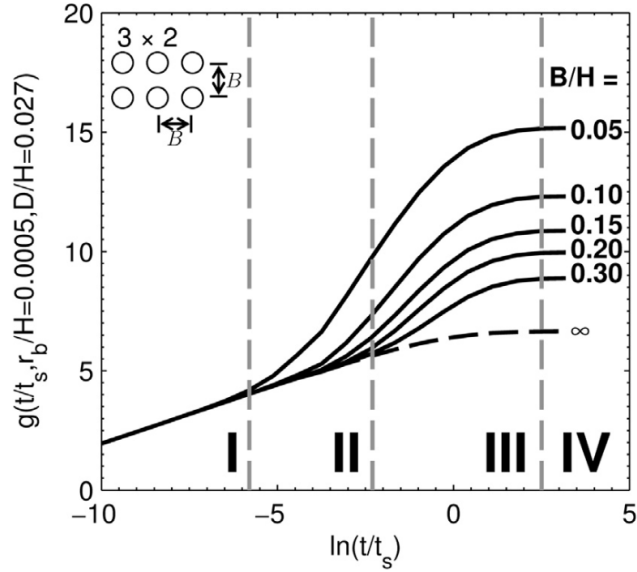


Figure 6.1: G-functions behavior [5]

As it is possible to deduce from figure 6.1 G-functions are presented in the form of dimensionless curves depending on dimensionless parameters as it is visible from equation 6.1 [38] [29]:

$$T_{ave}(r_b) = T_{gr} - \frac{\bar{Q}}{2\pi k_s} \cdot g \left(\ln(9Fo_H), \frac{r_b}{H}, \frac{B}{H} \right) \quad (6.1)$$

where

$$Fo_H = \frac{\alpha t}{H^2} \quad (6.2)$$

Fo_H is the Fourier number, defined as a function of the thermal diffusivity of the ground and of the borehole depth, and it provides information about the transient behavior of the BHEs field.

Then, each G-function is categorized into four distinct regions, each characterized by unique heat transfer attributes.

The estimation of the G-function is used to calculate the temperature drop at the borehole wall due to a constant heat extraction [29].

The borehole field used to validate the model consists of 6 boreholes arranged in a squared configuration in a 3×2 pattern.

This field possesses specific geometric characteristics and thermal properties summarized in the table below.

Heat transfer is exclusively taken into account within the vicinity of the boreholes, with no heat transfer calculations being conducted within the boreholes themselves. Consequently, the entire system comprises a single domain, encompassing both the borehole field and the adjacent surrounding ground.

Parameters	Value	Units
Borehole field		
Number of boreholes, N_b	6	-
Nominal borehole spacing	7.5	m
Borehole field		
Borehole depth, H	150	m
Borehole radius, r_b	0.075	m
Borehole buried depth, D	4	m
Thermal properties of the ground		
Undisturbed ground temperature T_0	6	°C
Ground thermal conductivity, κ_s	2	W/m·K
Ground thermal diffusivity, α_s	1e-6	m ² /s
Heat injection/extraction rate	12.57	W/m

Table 6.1: Parameters for model validation

The model is built in accordance with the properly BCs required by the FLS method, that involves ensuring a constant and consistent heat flux along the storage walls [25].

In the case under analysis, the initial temperature within the domain is established based on the typical undisturbed ground temperature in Norway, set at 8°C.

BCs in the surrounding domain are defined at considerable distances from the borehole field: radially at 150 meters and vertically below the borehole field at 200 meters. In these regions, temperatures are maintained at their undisturbed values of 8°C. Additionally, this temperature serves as a BC at the top surface of the domain [29].

To run simulations, the model exploits the heat transfer symmetry within the borehole field. Symmetrical boundaries are chosen carefully to ensure that the heat exchange between injection and extraction boreholes remains undisturbed. These symmetry boundaries are designated as adiabatic.

Since the previous BCs are required by the FLS method, results obtained by the numerical implementation of the analytical model proposed by Claesson and Javed should be compared with the FLS solution for a corresponding geometry featuring a 3×2 arrangement of

BHEs in a square pattern assuming: $\frac{r_b}{H} = 0.0005$ and $\frac{B}{H} = 0.05$. The simulation is run for $t = 20$ years, a sufficient duration to achieve a natural logarithm value of approximately -1.3 for $9Fo_H$ and a value of the G-function approximately equals to 11.9 °C as shown in figure 6.1 [38] [29].

If the model is correctly implemented, results regarding the thermal response function obtained from MATLAB must coincide with the theoretical ones.

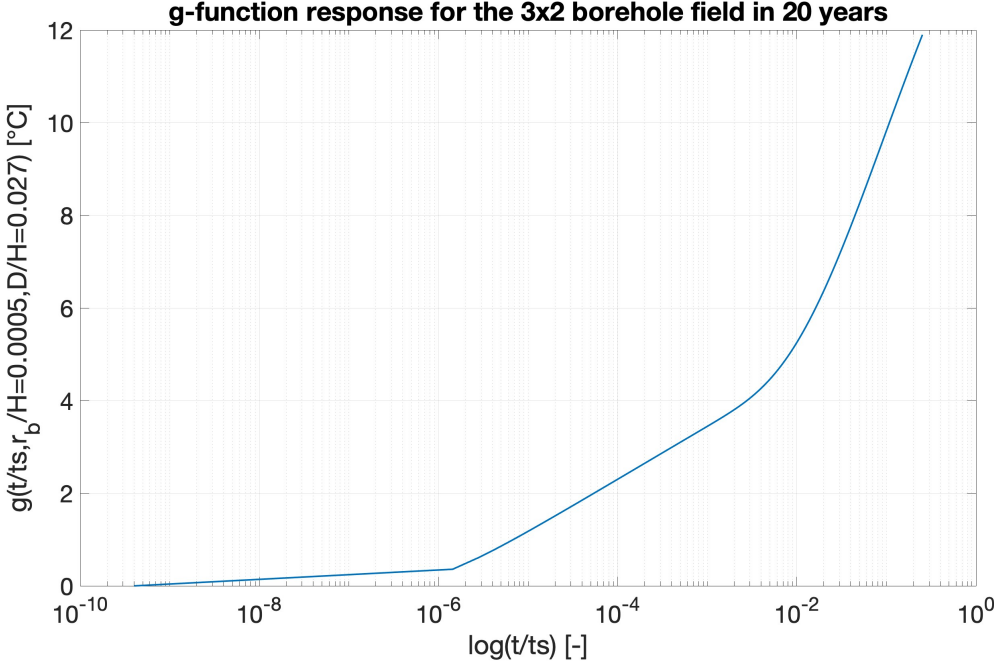


Figure 6.2: Validation from MATLAB simulation

Chapter 7

Results

In this chapter all the results concerning the design phase of the BTES are illustrated. In particular, the temperature profile of the average borehole wall temperature and the mean fluid temperature are analysed and discussed.

Then, sensitivity analysis is performed in order to understand which are the parameters that mostly affect the system performance.

Additionally, system behavior is analyzed considering the coupling of the storage with the HP under two different scenarios.

In conclusion, the heat losses is performed to estimate which storage parameter has an higher impact on the temperature's profiles.

It is worth noting that to provide a larger overview the analysis is carried out for two different types of load.

7.1 BTES Analysis

7.1.1 Results for Load 1

In accordance to the ASHRAE-Tp8 method, to obtain the average borehole wall temperature profile and mean water temperature profile inside the storage the surplus from the WIP must be evaluated.

Mathematically speaking, the previous concept can be synthesized in the following way:

$$E_{surplus/deficit} = E_{WIP} - E_{LTDH} \quad (7.1)$$

The surplus is defined as the difference between what comes from the WIP and the demand from the LT-DH monthly based.

In particular, since for the LT-DH data are provided on hourly basis to pass to the desired values, the hour information are averaged over the months.

In this context, the most significant information can be extracted from energy calculations. Results are presented below:

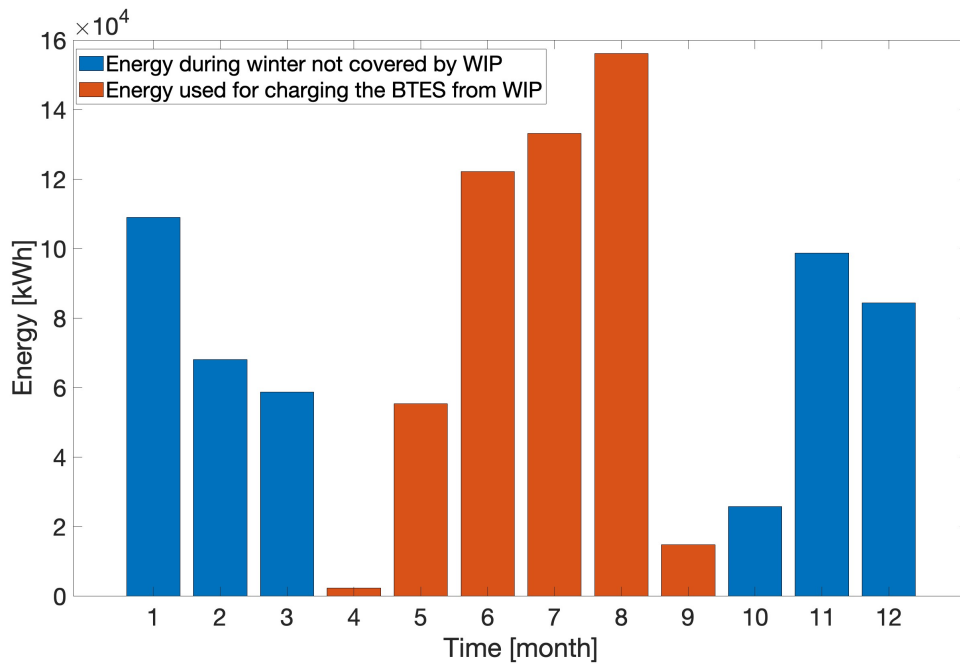


Figure 7.1: Surplus and deficit for Load 1

As it is possible to deduce from figure 7.1, blue colored bars represent the deficit during the winter season. In particular, during this period the load from the LT-DH is higher than the energy from the WIP and according to equation 7.1 the BTES is in discharging mode because it is used to supply the required energy to the LT-DH network.

In contrast, red colored bars represent the surplus during the summer. In fact, during this season the amount of energy from the WIP is higher compared to the LT-DH demand and the excess is used to charge BTES.

Once this analysis has been performed, by implementing the load aggregation algorithm it is possible to evaluate the main temperatures profiles', as it is shown in figure 7.2.

In this figure the storage behavior is highlighted:

- during the winter season, the heat is transferred from the storage to the fluid causing a temperature increase on the way towards the DH. A further fluid temperature

increase is due to the heat pump present in between the two subsystems. This season corresponds to the discharging phase of the BTES.

- during the summer season when the storage is charged, it is possible to observe a gradual increase of the temperatures both of the wall and of the fluid but the directionality of the heat transfer is from the fluid towards the storage wall.

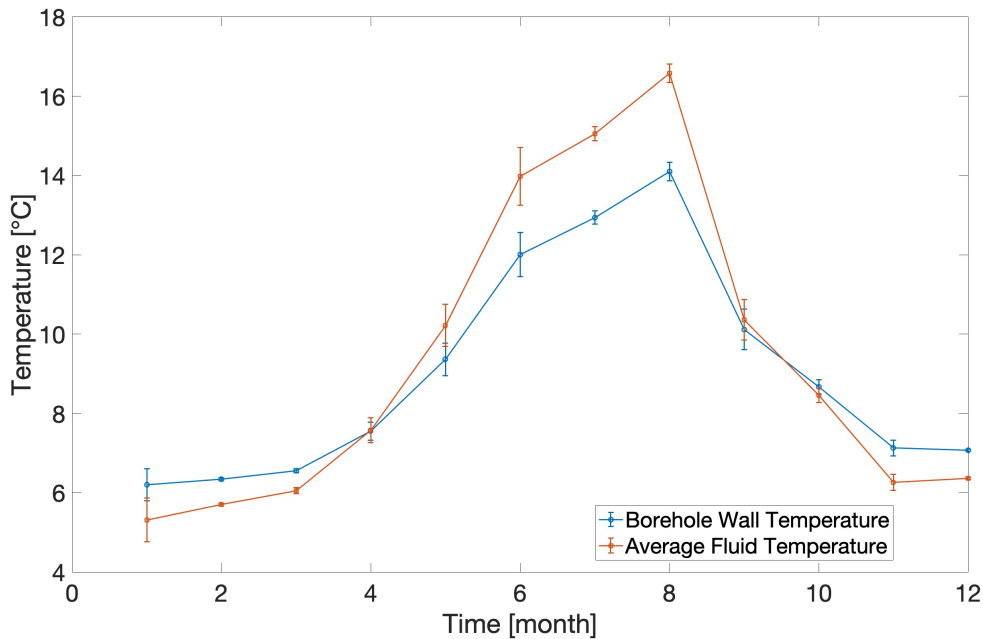


Figure 7.2: Average borehole wall temperature and mean fluid temperature for Load 1

It is important to notice that the dynamic behavior of the BTES in each month is partially considered.

Specifically, for each month the graph shows the presence of error bars that are computing by calculating the mean values and the temperatures' standard deviations.

Based on the calculated monthly means and standard deviations, the maximum and minimum values are determined to define the error bands of borehole wall temperature and average water temperature.

These bands represent the range within which the above mentioned temperatures can vary with a certain probability within each month.

7.1.2 Results For Load 2

Results for Load 2 are the same obtained for Load 1 but the temperature and energy levels are different.

Although the trend of the graphs mirror the situation of Load 1 some discrepancies are present.

Firstly, with reference to figure 7.3 the amount of charging and discharging energy is high because keeping constant the energy rate produced from the WIP and being the demand from LT-DH lower the resulting deficit and surplus is higher.

Secondly, according to figure 7.4 it is possible to notice that the borehole wall temperature and the average water temperature are higher compared to the temperature profiles' of the previous case during the charging phase as a consequence of the high amount of energy that can be stored. While the temperature values during the discharging phase are lower compared to Load 1 because of the higher amount of energy that can be discharged.

The observation done for temperature profiles in case of Load 1 are still valid for Load 2 and they are evident in figure 7.4.

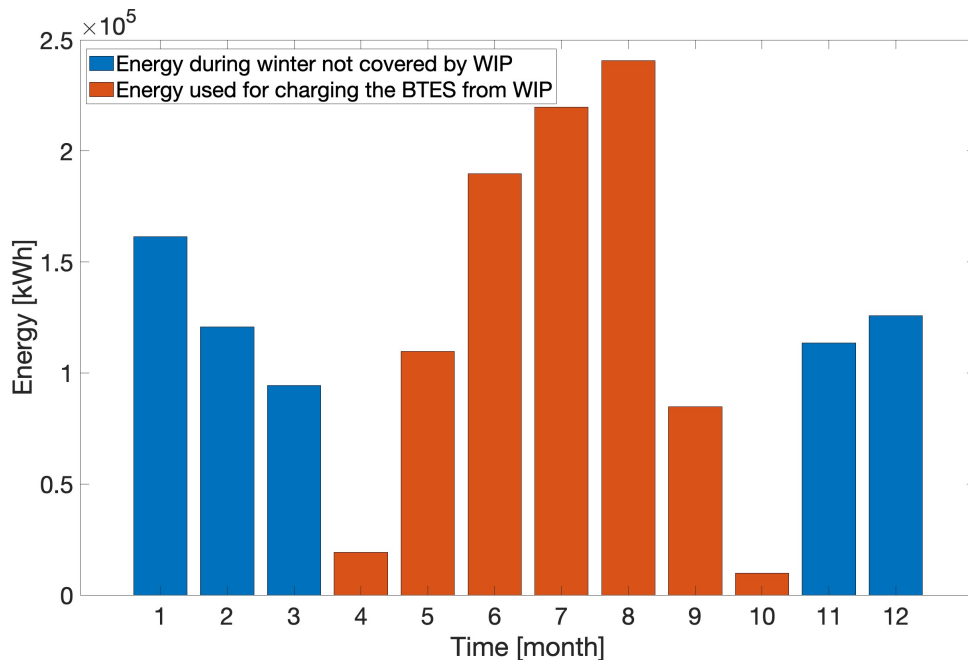


Figure 7.3: Surplus and deficit for Load 2

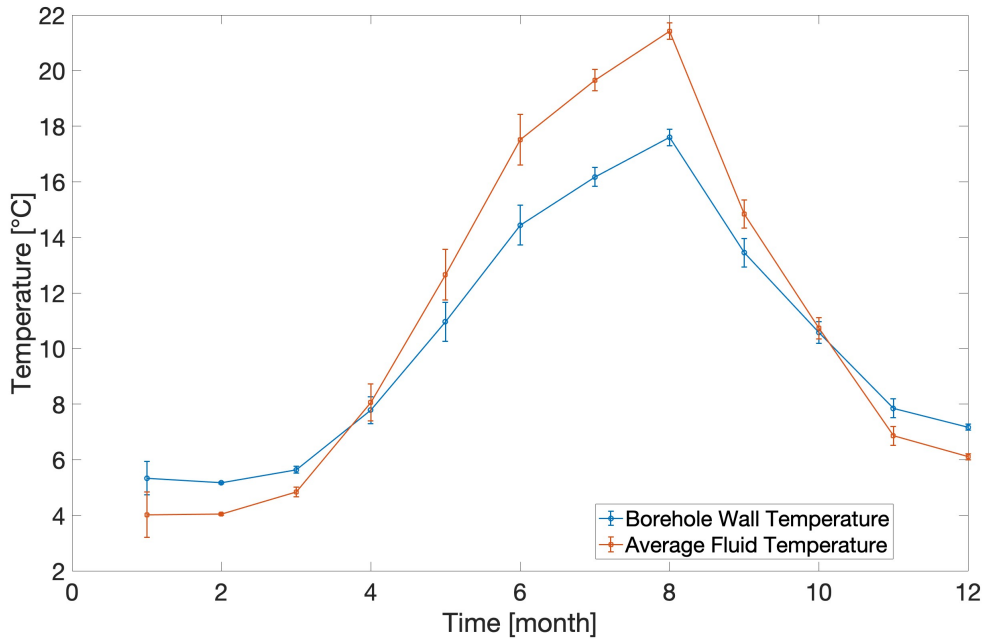


Figure 7.4: Average borehole wall temperature and mean fluid temperature for Load 2

7.2 Sensitivity Analysis

Sensitivity analysis is a fundamental technique used to assess the impact of parameter variations on the system performance.

Its primary objective is to understand how changes in input parameters affect the output or performance of a model, simulation, or process.

There are several methods and approaches used to conduct the sensitivity analysis, each tailored to different types of models and objectives.

In this thesis, the approach involved is the so called *One-at-a-Time (OAT) Sensitivity Analysis* technique.

This method entails varying one parameter at a time while keeping all the others constant, allowing for the isolation of individual parameter effects on the system's response.

Despite its simplicity and intuitiveness, this technique may lead to neglect interactions between parameters.

In this thesis, the sensitivity analysis is performed in order to evaluate which is the impact of the main storage parameters on the system's performance. Main parameters analyzed are: *borehole depth, borehole radius, number of BHEs, BHEs distance, thermal conductivity of backfilling material, thermal conductivity of the ground and HP's COP.*

7.2.1 Sensitivity Analysis Load 1

The evaluation of the sensitivity analysis is focused on how the borehole wall temperature and mean fluid temperature vary according to a precise variation of the storage parameters.

It is worth noting that the variation of the single parameters is not casual but it is accurately chosen and referenced.

7.2.1.1 Sensitivity to the borehole depth

The sensitivity to the borehole depth is illustrated in figure 7.5.

The borehole depth represents a fundamental parameter because it is strictly related to the investment costs of the plant itself. In fact, it directly affects the equipment used for drilling operations and limitations imposed by geological factors [39].

As demonstrated by the existing plants, the borehole length falls in the range 40 m to 500 m but a good trade-off between thermal losses and costs is the range 150 m to 250 m[40].

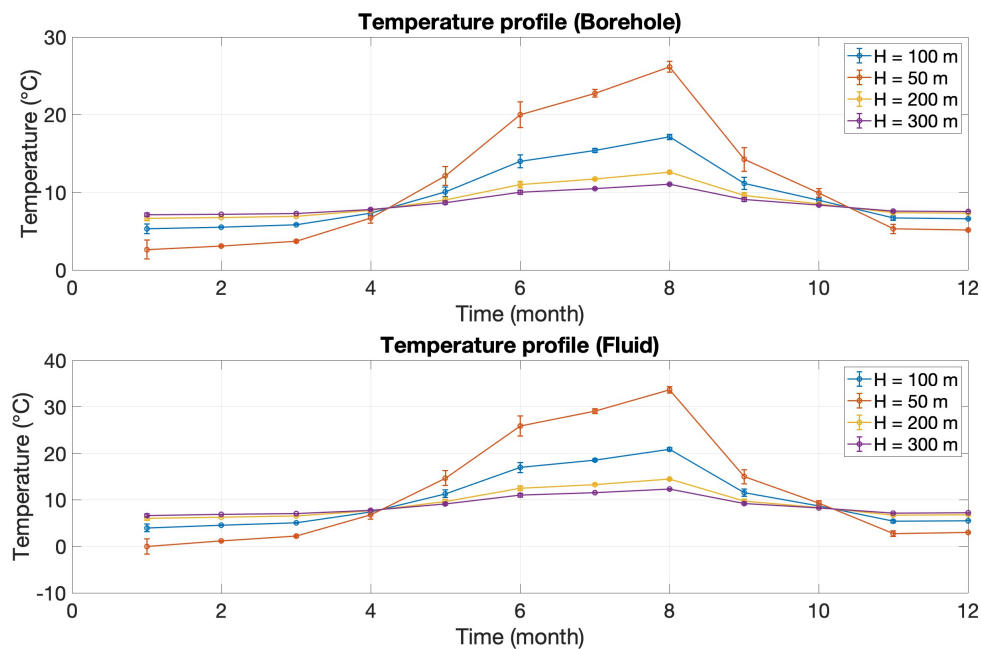


Figure 7.5: Sensitivity to the borehole depth for Load 1

As it is visible from the figure 7.5, at 50 m both the borehole wall temperature and the average fluid temperature show a different trend in comparison to the other cases.

This behavior can be justified referring to the amount of heat exchanged. In particular, at reduced depths the BHEs is neither able to provide a sufficient amount of energy nor to absorb it. So, during the discharging period both the temperatures are in average lower while during the charging season they are higher.

In other words, reducing the storage capacity but keeping constant the amount of energy stored it is possible to observe an increase in terms of temperatures.

It is worth noting that the temperature increase is not linear.

7.2.1.2 Sensitivity to the *Borehole Radius*

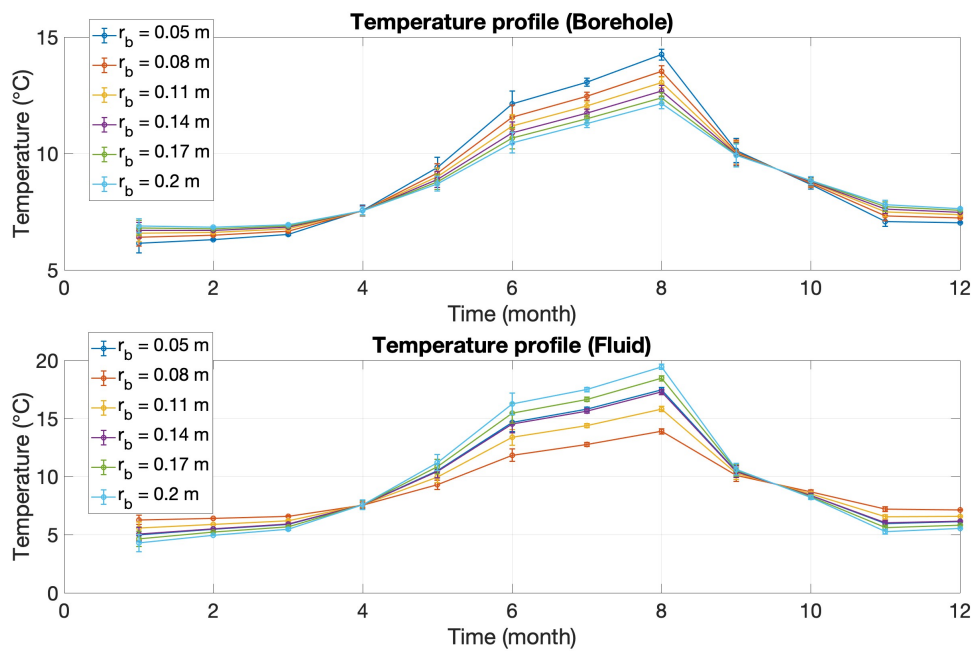


Figure 7.6: Sensitivity to the borehole radius for Load 1

As the borehole depth also the borehole radius has a strong influence on the investment costs of the plant because it is strictly related to the drilling technique adopted.

Regarding the temperature profiles obtained from MATLAB simulations it is possible to deduce that changing the storage radius has a direct implication on the variation of the storage capacity. Being the sensitivity analysis performed only one parameter at once, keeping constant the amount of energy stored or delivered the result is a decrease of the

temperatures during the discharging period while there is an increase during the charging period.

7.2.1.3 Sensitivity to the *Number Of BHEs*

The number of BHEs installed in a specific site must ensure that it covers the heating demand from the LT-DH network.

For this reason, starting from a minimum acceptable number of BHEs it is only possible to increase the amount of heat exchangers.

From figure 7.7 it is immediately noticeable that highly increasing the storage capacity by increasing the number of BHEs a plateau is reached.

This behavior can be explained by considering that since the BTES model takes into consideration not only the interactions between the BHEs and the ground but also the interactions among the BHEs field at a certain point being the number of BHEs significantly high a thermal equilibrium between them and the surrounding ground is obtained.

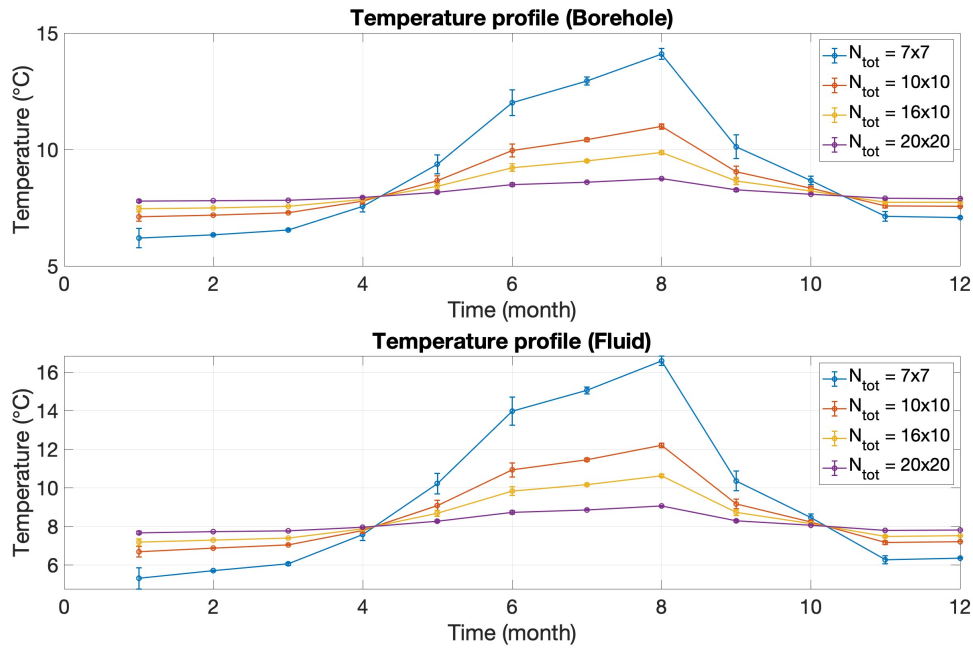


Figure 7.7: Sensitivity to the number of BHEs for Load 1

7.2.1.4 Sensitivity to the *BHEs Distance*

As it is visible from figure 7.8, borehole wall temperature and average fluid temperature significantly vary as the distance between the heat exchangers decreases.

This effect is due to the excessively interference between the BHEs that causes them to highly interact during the charging period with the consequence of an uncontrolled temperature increase during this period.

On the other hand, during the discharging period BHEs poorly interact among each other causing a an abrupt temperature decrease.

Typically, it has been observed that ideal BHEs distances are in the range between 3 m to 8 m because this is the minimum acceptable range such that BHEs interactions' do not have a catastrophic effect on the storage temperatures [40].

Moreover, according to figure 7.8 and according to the previous observation it is clear that increasing the distance between BHEs temperature profiles tend to a uniform trend being the interactions between them non prevailing.

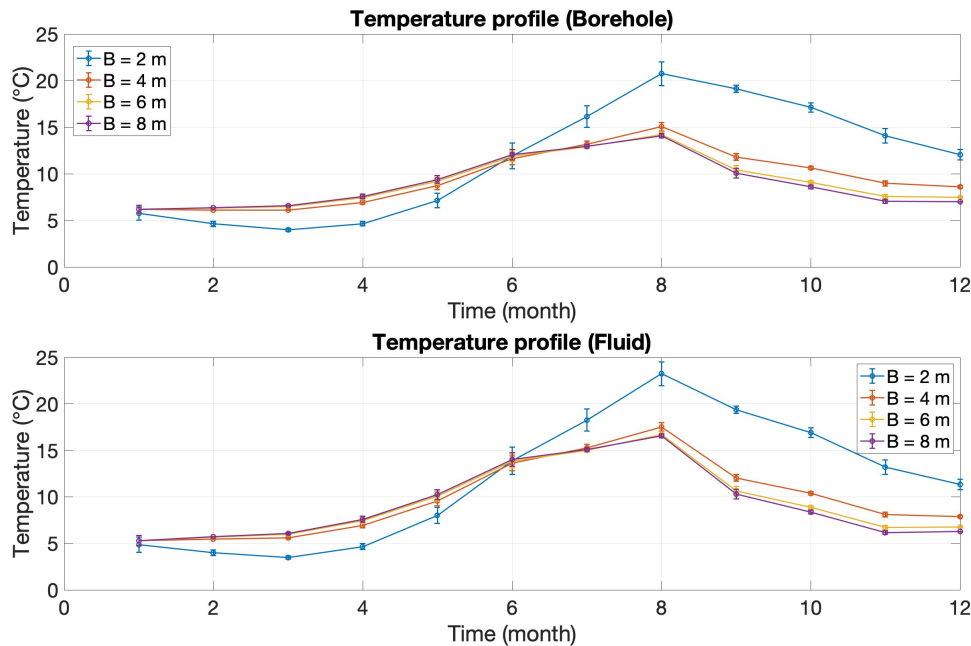


Figure 7.8: Sensitivity to the BHEs distance for Load 1

7.2.1.5 Sensitivity to *Thermal Conductivity of the Backfilling Material* k_{fill}

The usage of the sand-bentonite as backfilling material for grouted BHEs is used to enhance the heat exchange mechanism inside the storage itself if compared to the effect of the traditional sand-clay material [41].

As it is visible from the figure 7.9 the value of the thermal conductivity of the backfilling material varies in a wide range from 0.5 to $2.5 \frac{W}{mK}$.

Particularly, experimental values for sand-bentonite materials show that thermal conductivity falls in the range from 2.15 to $2.38 \frac{W}{mK}$ while lower values are typical of sand-clays materials [41].

Specifically referring to the figure below it is possible to deduce that the borehole temperature profile is not affected by the value of k_{fill} being only a function on the thermal conductivity of the ground k_g . On the other hand, the temperature profile of the average fluid temperature is influenced by the value of k_{fill} in such a way that in presence of sand-bentonite materials being the heat injection and extraction enhanced temperature levels are lower if compared to the values reached in presence of typical sand-clays materials.

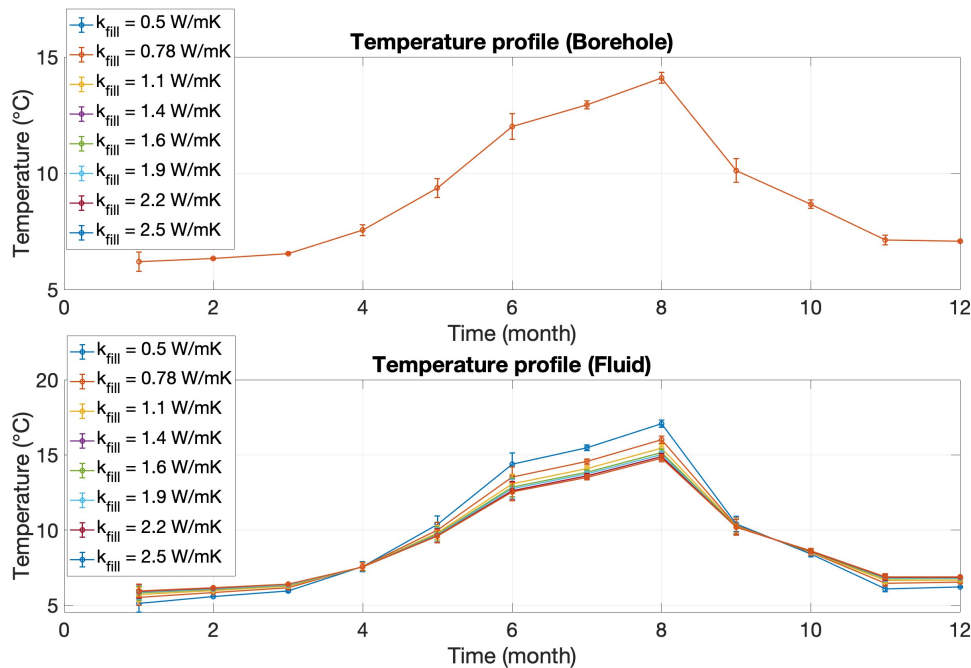


Figure 7.9: Sensitivity to k_{fill} for Load 1

7.2.1.6 Sensitivity to *Thermal Conductivity of the Ground* k_g

The value of the thermal conductivity of the ground is strictly related to the geographical location where the storage system is installed.

In this study, values used to run the simulations have been taken from experimental in-situ tests performed in Norway. So, these values are typical of Norwegian regions [42].

Generally, k_g mainly affects the investment costs and the heat exchanger rate inside the storage.

Firstly, according to the type of soil in which the plant is installed the drilling technique involved varies and especially in presence of unconsolidated sediments and hard rocks the necessity of specific and costly techniques is required.

Secondly, through k_g it is possible to quantify the heat exchange rate between the ground itself and the water inside the boreholes according to the thermal response function.

In particular, higher the value of k_g lower is the value of the G-function and consequently, higher are the temperature levels.

With a particular reference to the figure 7.10 when the value of k_g increases both borehole wall temperature and average water temperature decrease with a non linear trend.

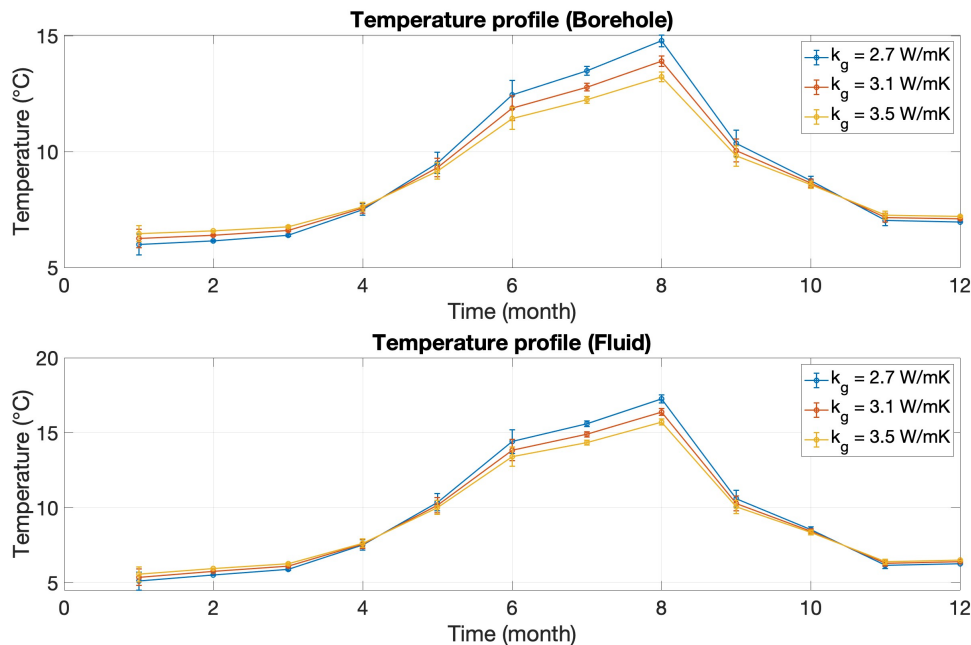


Figure 7.10: Sensitivity to k_g for Load 1

7.2.1.7 Sensitivity to *HP's COP*

One of the most critical choice to be made during the design phase of this plant is the heat pump selection that strictly influences the operating costs through its coefficient of performance COP [43].

For well-designed systems the HP's COP should be ideally adjusted to the temperature coming from the BTES being the two systems directly connected.

With a particular reference to this work, the HP's COP is evaluated starting from two fixed temperature levels such that they guarantee a minimum acceptable COP for these applications of 2. Moreover, this parameter is only involved during the discharging phase of BTES in order to adjust the amount of heat extracted from the storage and to ideally provide an additional boost to the outlet water temperature from the BTES.

As highlighted by Croteau et al. (2015) in their work HP's COP should be in the range 2 to 7.5 to be a good trade-off between the system performance and operational costs [43].

From the analysis of figure 7.11 it is possible to note that since in this thesis the heat pump is not thermally coupled to the storage system, temperatures' profiles are not eminently affected by the HP's COP.

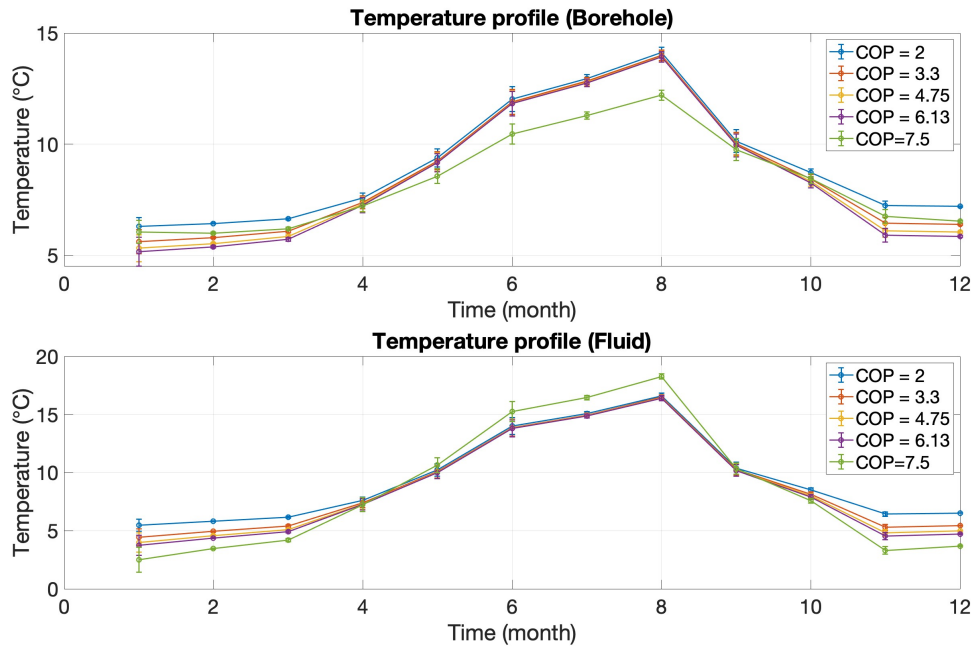


Figure 7.11: Sensitivity to HP's COP for Load 1

In this context, the analysis is carried out by using the regression model for the HP.

7.2.1.8 Sensitivity Analysis Results' Summary

In this section, a result summary of the sensitivity analysis is presented. In particular, it is worth analyzing which are the parameters that mostly affect the sensitivity analysis in case of Load 1.

In other word, figure 7.12 shows which of the previous parameters have major impacts on system performance.

In this specific case, the most crucial parameters are: the borehole depth and the distance between the boreholes because they are responsible for the highest temperature deviation from the base case.

The evaluation of the most critical parameters is based on the calculation of the average temperatures and then the deviation from the base case is contained inside the ΔT .

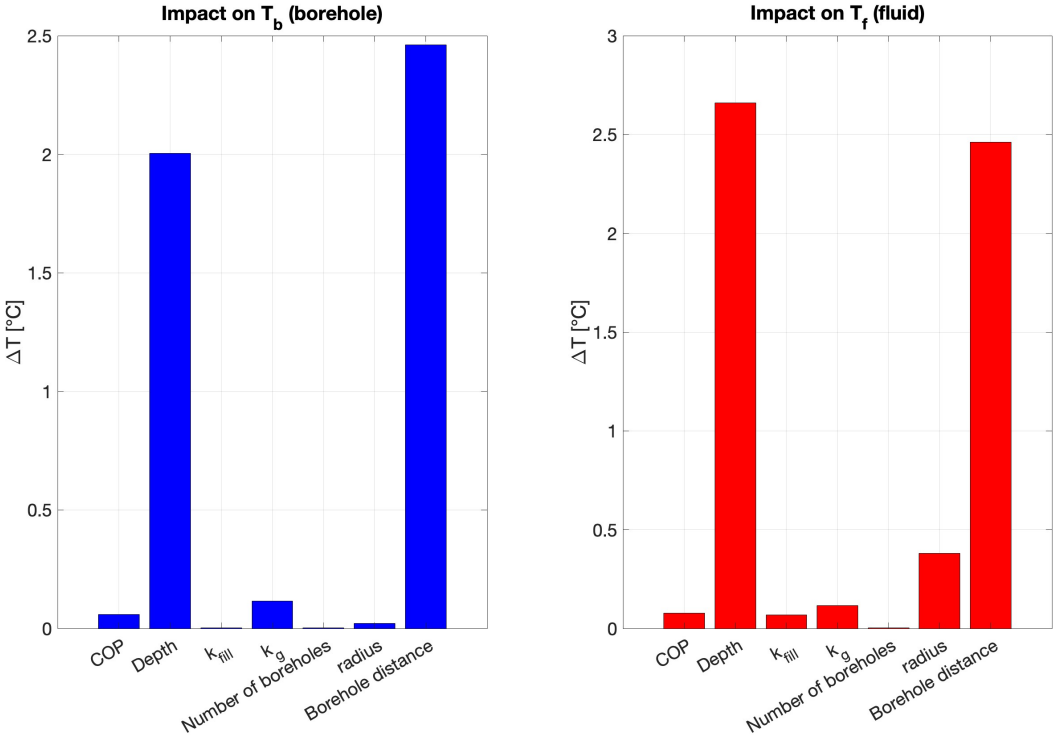


Figure 7.12: Sensitivity impact for Load 1

7.2.2 Sensitivity Analysis Load 2

In this section, results concerning the sensitivity analysis of Load 2 are contained. Principles below this analysis are the same as Load 1 but results are slightly different.

7.2.2.1 Sensitivity to the *Borehole Depth*

The sensitivity to the borehole depth is illustrated in figure 7.13.

As for Load 1, also in case of Load 2 the variability range chosen is 50 m to 300 m and as it is visible from the figure below at 50 m both the borehole wall temperature and the average fluid temperature show a different trend in comparison to the other cases.

This behavior can be justified referring to the amount of heat exchanged and to the storage capacity.

In particular, reducing the storage capacity due to the depth reduction but keeping constant the amount of energy stored it is possible to observe an increase in terms of temperatures and the temperature increase is not linear.

In conclusion, at reduced depths the BHEs is neither able to provide a sufficient amount of energy nor to absorb it. So, during the discharging period both the temperatures are in average lower while during the charging season they are higher.

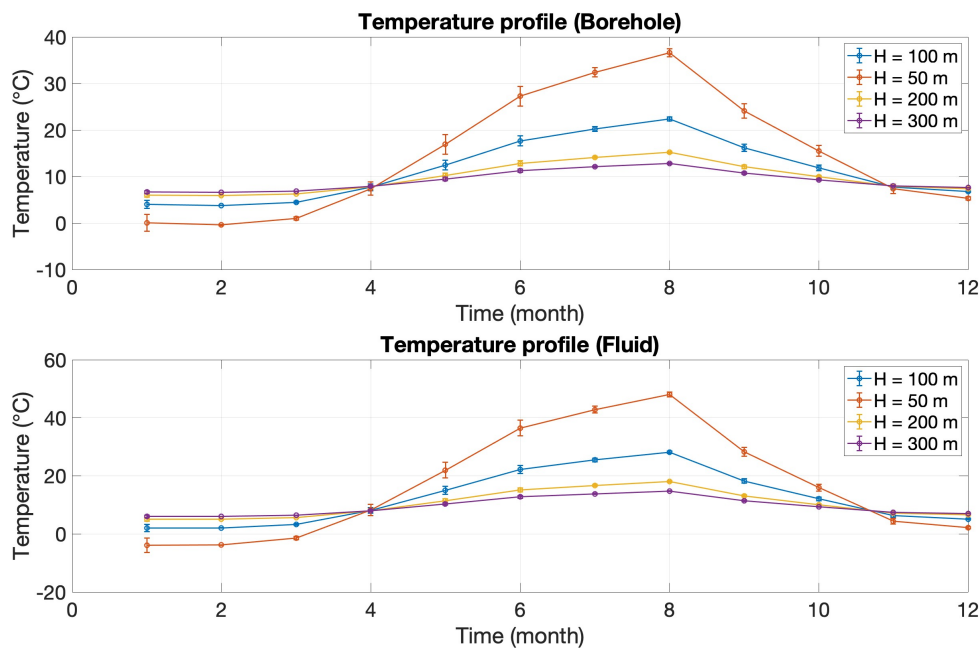


Figure 7.13: Sensitivity to borehole depth for Load 2

7.2.2.2 Sensitivity to the *Borehole Radius*

From MATLAB simulations it has been possible to deduce that changing the storage radius has a direct implication on the variation of the storage capacity.

Being the sensitivity analysis performed only one parameter at once, keeping constant the amount of energy stored or delivered the result is a decrease of the temperature levels during the discharging period while there is an increase during the charging period.

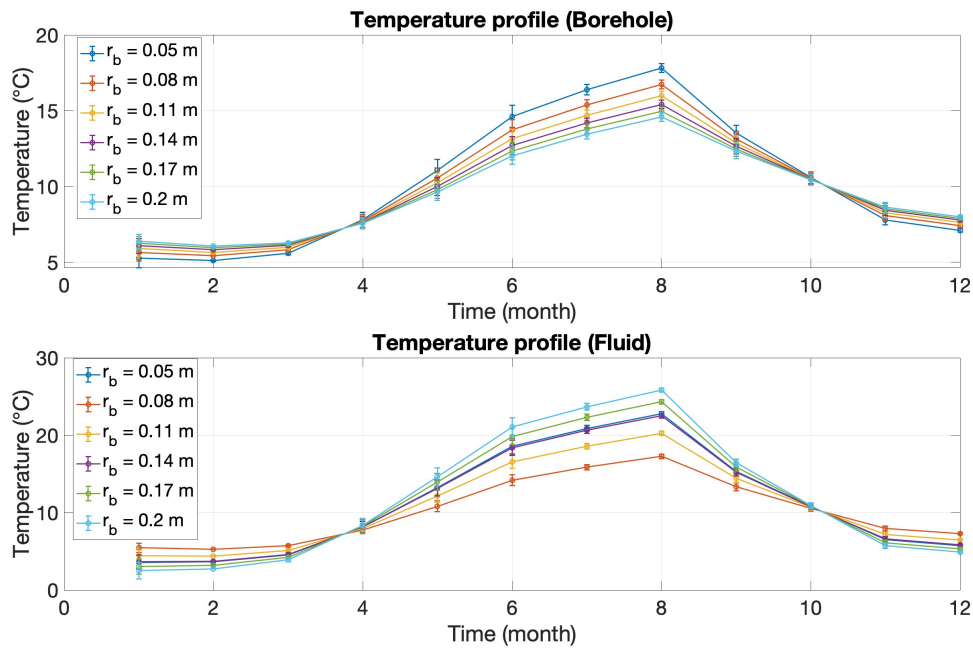


Figure 7.14: Sensitivity to borehole radius for Load 2

7.2.2.3 Sensitivity to the *Number of BHEs*

From figure 7.15 it is possible to notice that highly increasing the storage capacity by increasing the number of BHEs a plateau is reached.

This behavior can be explained by considering that since the BTES model takes into consideration not only the interactions between the BHEs and the ground but also the interactions among the BHEs field at a certain point being the number of BHEs significantly high a thermal equilibrium between them and the surrounding ground is obtained.

As for Load 1, even in this case different configurations are explored, specifically not only perfectly squared but also rectangular configurations are analyzed.

Final results show that the thermal effects on non-perfectly squared configurations are

the same of squared configurations.

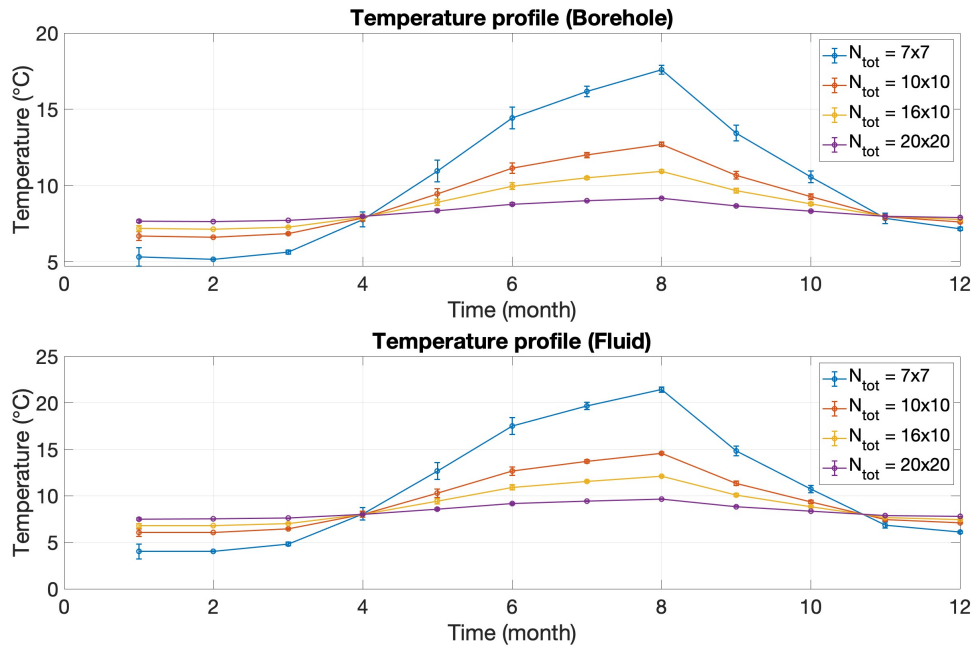


Figure 7.15: Sensitivity to number of BHEs for Load 2

7.2.2.4 Sensitivity to the *BHEs* Distance

As for Load 1 also in this case borehole wall temperature and average fluid temperature significantly vary as the distance between the heat exchangers decreases.

This effect is due to the excessively interference between the BHEs that causes them to highly interact during the charging period with the consequence of an uncontrolled temperature increase during this period.

On the other hand, during the discharging period BHEs poorly interact among each other causing a an abrupt temperature decrease. In this case, it is possible to observe temperature levels even lower than 0 °C.

Moreover, according to figure 7.16 and according to the previous observation it is clear that increasing the distance between BHEs temperature profiles tend to a uniform trend being the interactions between them non prevailing.

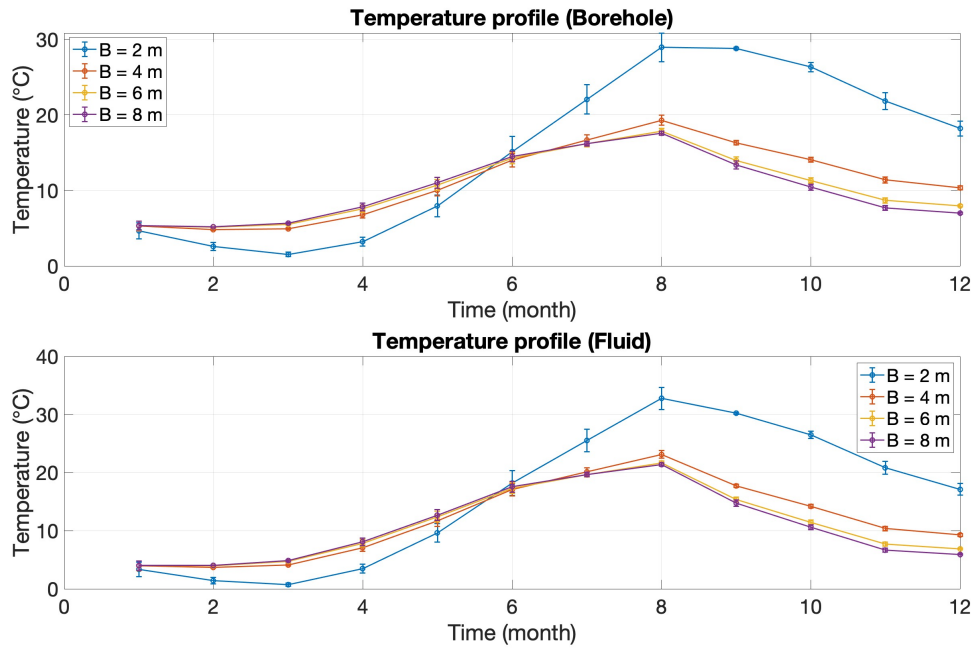


Figure 7.16: Sensitivity to the distance between BHEs for Load 2

7.2.2.5 Sensitivity to the *Thermal Conductivity of the Backfilling Material* k_{fill}

As for Load 1 also for Load 2 the range of k_{fill} explored takes into consideration thermal conductivity of both traditional sand-clay materials and sand-bentonite materials, specifically from $0.5 \frac{W}{mK}$ to $2.5 \frac{W}{mK}$.

With a particular reference to the figure below it is possible to deduce that the borehole wall temperature profile is not affected by the value of k_{fill} being only a function of the thermal conductivity of the ground k_g . On the other hand, the temperature profile of the average fluid temperature is influenced by the value of k_{fill} in such a way that in presence of sand-bentonite materials being the heat injection and extraction enhanced temperature levels are lower if compared to the values reached in presence of typical sand-clay materials.

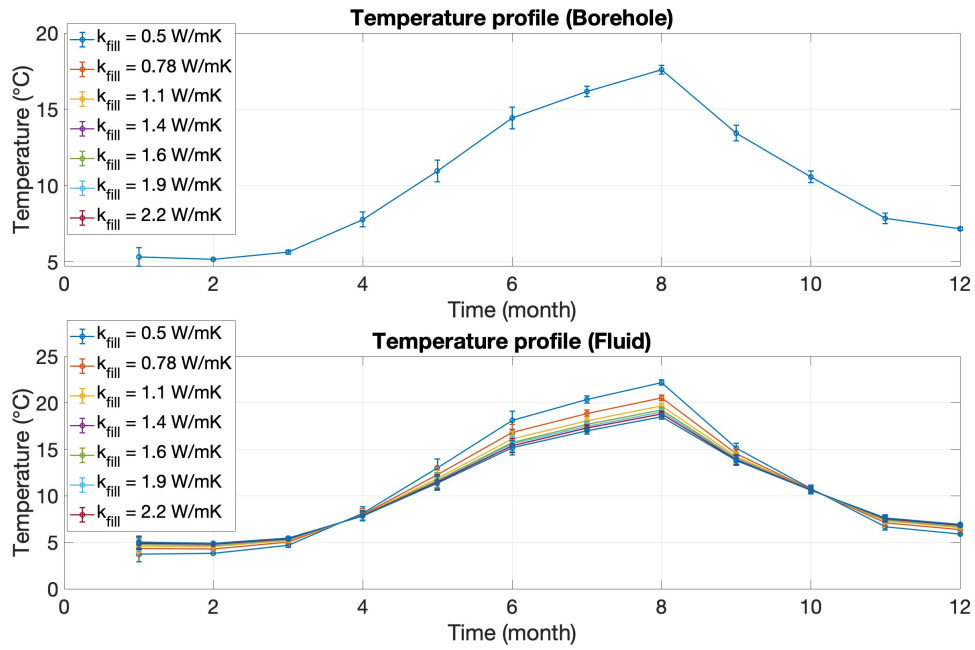


Figure 7.17: Sensitivity to k_{fill} for Load 2

7.2.2.6 Sensitivity to the *Thermal Conductivity of the Ground* k_g

As shown in the figure 7.18 when the value of k_g increases both borehole wall temperature and average water temperature decrease with a non linear trend.

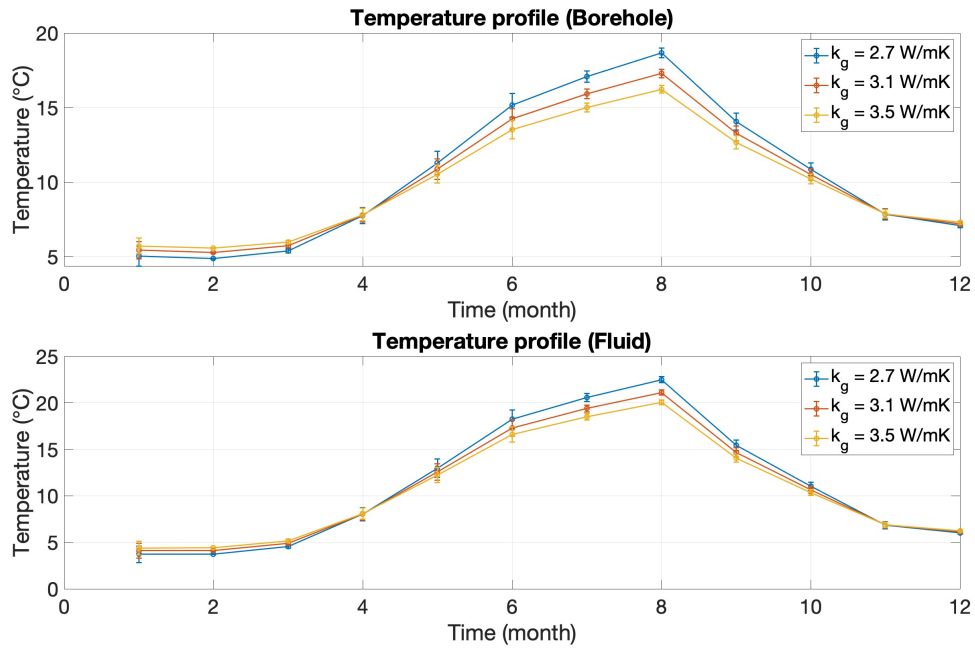


Figure 7.18: Sensitivity to k_g for Load 2

7.2.2.7 Sensitivity To *HP's COP*

As for Load 1 also for Load 2 from the analysis of figure 7.19 it is possible to note that since in this thesis the heat pump is not thermally coupled to the storage system, temperatures' profiles are not eminently affected by the HP's COP.

Also in this case it is worth noting that the sensitivity analysis is performed considering the regression model approach for the heat pump modeling.

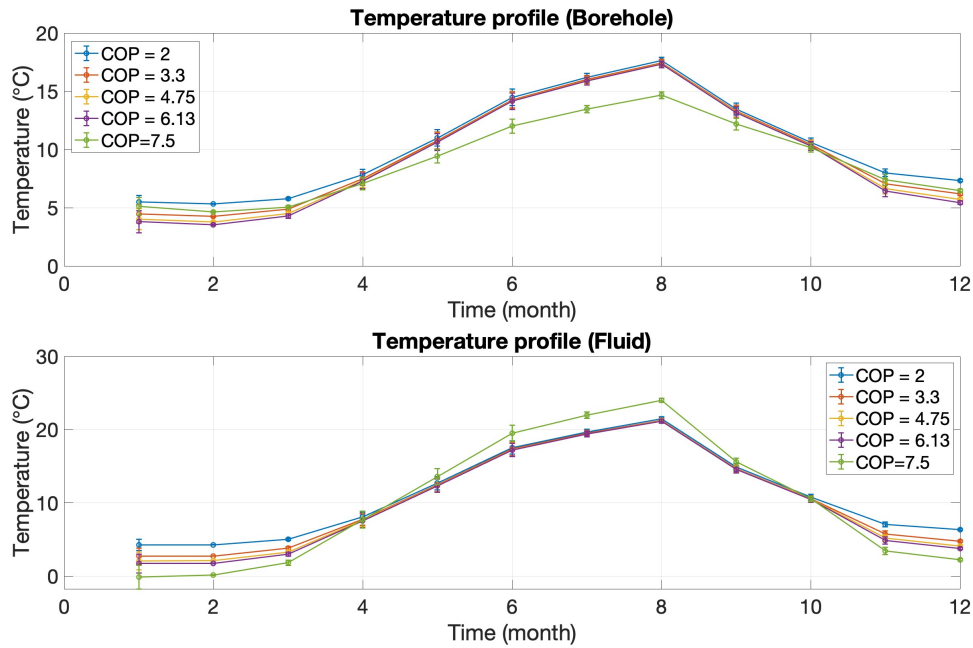


Figure 7.19: Sensitivity to HP's COP for Load 2

7.2.2.8 Sensitivity Analysis Results' Summary

In this section, a result summary is presented. In particular, it is worth analyzing which are the parameters that mostly affect the sensitivity analysis in case of Load 2.

In other word, figure 7.20 shows which of the previous parameters have major impacts on system performance.

As for Load 1 also for Load 2 the most crucial parameters are: the borehole depth and the distance between the boreholes because they are responsible for the highest temperature deviation from the base case.

The evaluation of the most critical parameters is based on the calculation of the average temperatures and then the deviation from the base case is contained inside the ΔT .

Comparing the results obtained for Load 2 with the results obtained for Load 1 the resulting ΔT values are higher for Load 2. This is mainly due to the higher amount of energy stored.

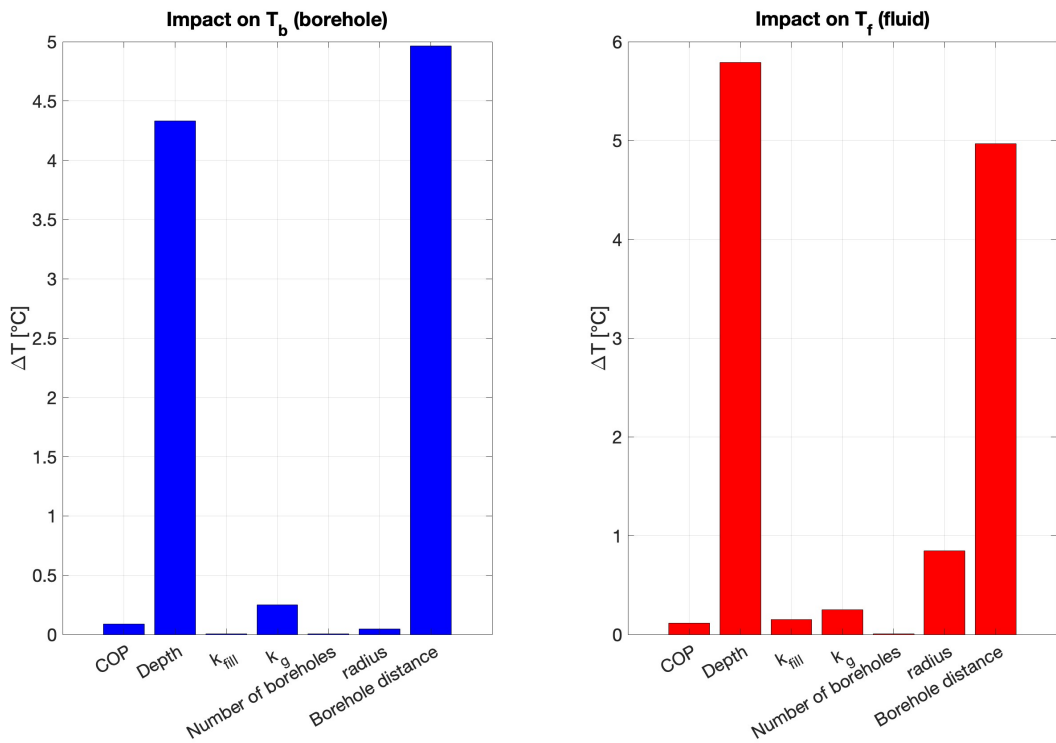


Figure 7.20: Sensitivity impact on BTES performances for Load 2

7.3 Long-term Storage Performances

This section has the aim of analyzing the effects of dynamic temperature variations within the storage system under two different scenarios: firstly, when it is uniquely subject to a charging period, and secondly, when experiencing a cycling pattern of charging and discharging period after a period of only charging.

Such analysis is fundamental for the understanding of system's behavior on long-term and to have a comprehensive insight into the thermal response of the storage system under different operating conditions.

7.3.1 5 Years of Only Charging

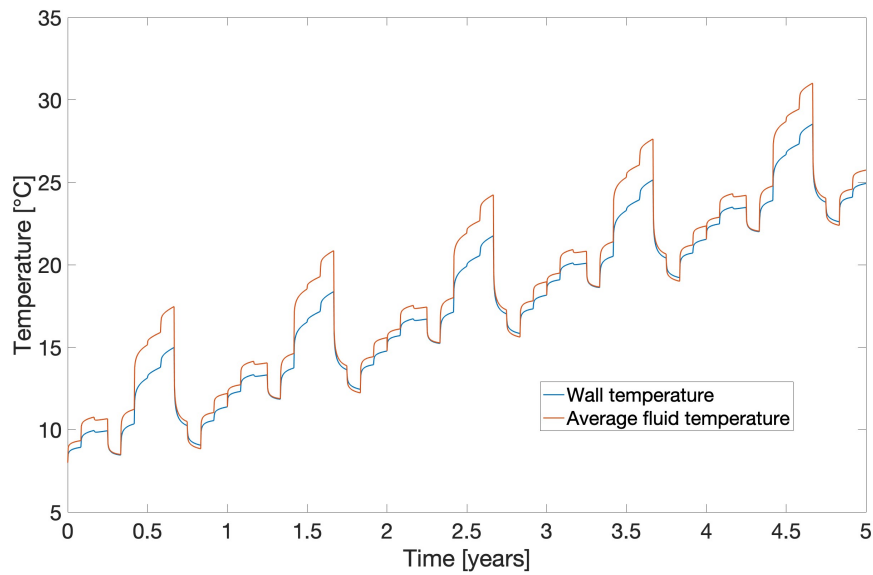
Figure 7.21 shows the behavior of the storage system when it is subject to a period of 5 years of only charging.

As it is visible, even if cycles of charging and discharging are realized annually the global trend is an increasing trend because the amount of energy charged is higher in comparison

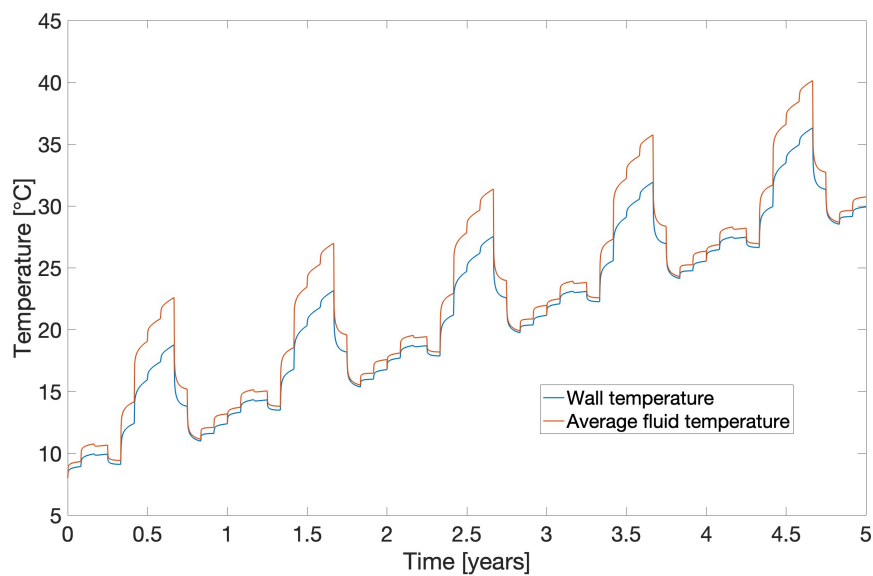
with amount of energy discharged that has been set equal to zero.

The main difference between Load 1 and Load 2 is expected in terms of temperature levels reached at the end of the overall charging period.

For Load 1, in fact, since the annual energy stored is higher in comparison to Load 2 at the end of the charging period the storage is expected to have higher temperatures.



(a) Load 1

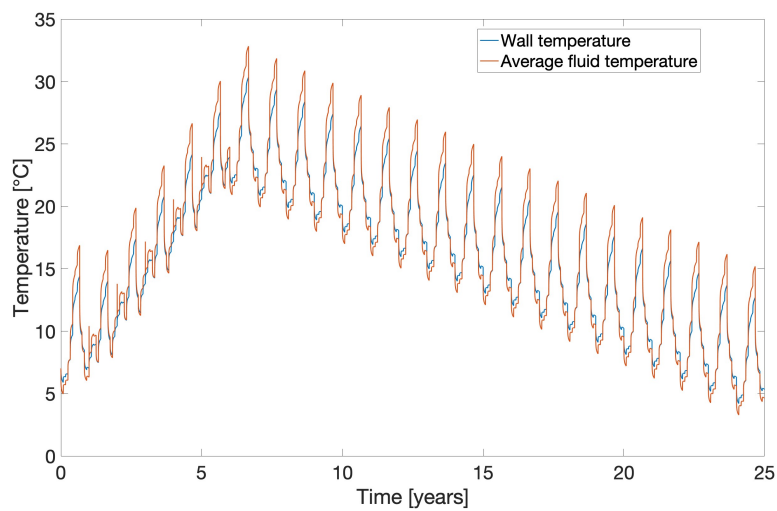


(b) Load 2

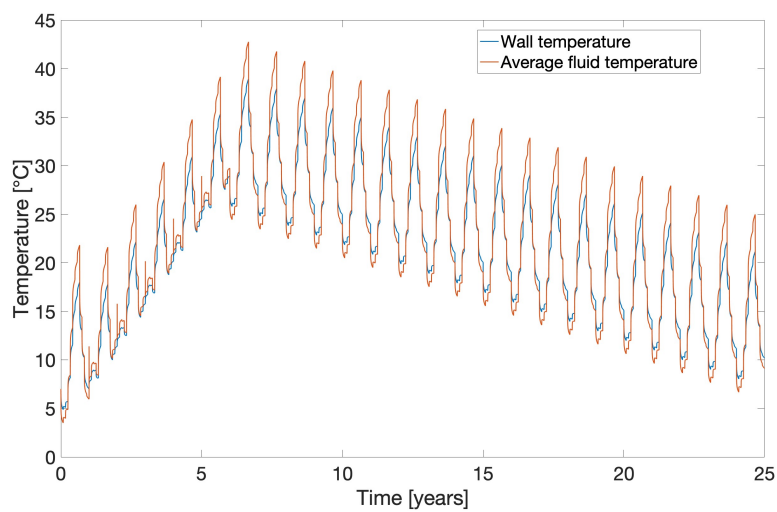
Figure 7.21: 5 years of only charging comparison

7.3.2 5 Years of Only Charging and 20 Years of Charging and Discharging

Figure 7.22 shows the system behavior when it is subject to a period of 5 years of only charging and then to a period of 20 years of periodic charging and discharging. As discussed in Section 7.3.1, since for the first 5 years the storage is only subject to a charging phase the overall trend is increasing. When the 20 years-period of charging and discharging starts the overall trend is a decreasing trend meaning that the amount of energy discharged is higher in comparison to the amount of charging energy. If an energy balance between the charging and discharging energy were reached, temperature levels would be assessed at a constant temperature.



(a) Load 1



(b) Load 2

Figure 7.22: 5 years of only charging and 20 years of charging and discharging comparison

7.4 Heat Losses Evaluation

Heat losses evaluation is one of crucial point for every seasonal thermal energy storage. In a BTES losses mainly depends on the storage volume and the temperature levels reached inside the storage itself.

The aim of this section is only to provide a rough estimation of energy losses in the storage system under analysis. For this reason, the quantitative results obtained are realistic and provide an information about the order of magnitude of expected losses but they are not precise.

Firstly, the storage volume has been evaluated according to the following formula:

$$Volume = B^2 \cdot N_{tot} \cdot H \quad (7.2)$$

where B is the distance between one borehole and the subsequent, N_{tot} is the total number of boreholes and H is the BHEs length.

Secondly, the energy in the ground has been evaluated according to the equation 7.3:

$$E_{ground} = m \cdot c_p \cdot \Delta T \quad (7.3)$$

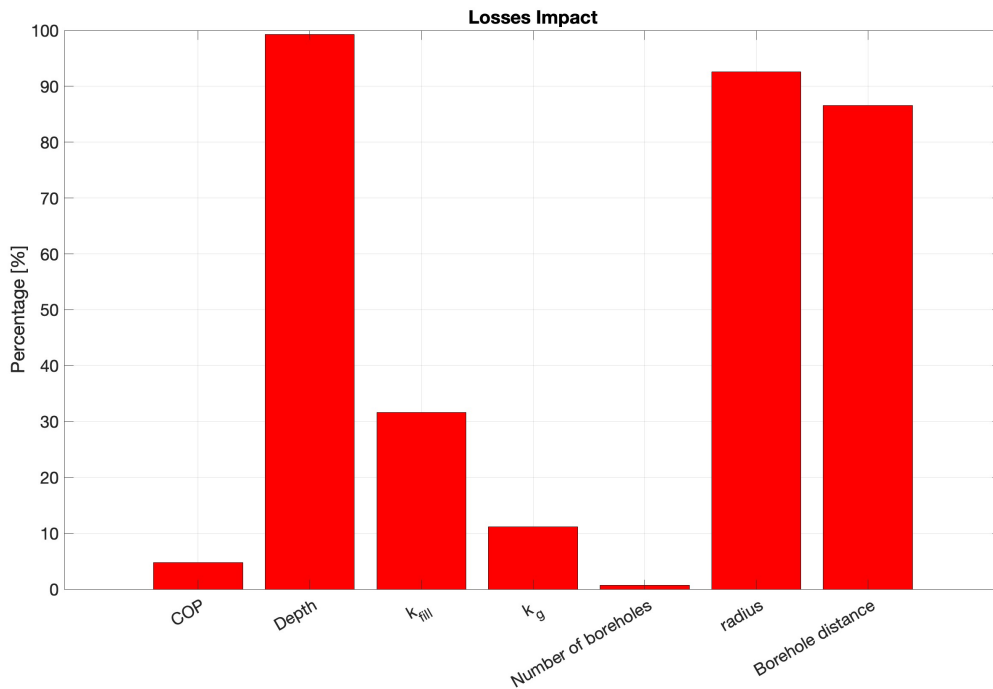
where m is the mass of the ground c_p is the thermal capacity of the ground and ΔT is the temperature difference observed in the ground, evaluated as the difference between the initial and the final values of the borehole wall temperature.

Finally, the amount of charging and discharging energy are calculated respectively as the excess from the waste incineration plant from April to October and as the deficit from January to March and from November to December evaluated considering the amount of energy that cannot be supplied by the WIP to the DH network.

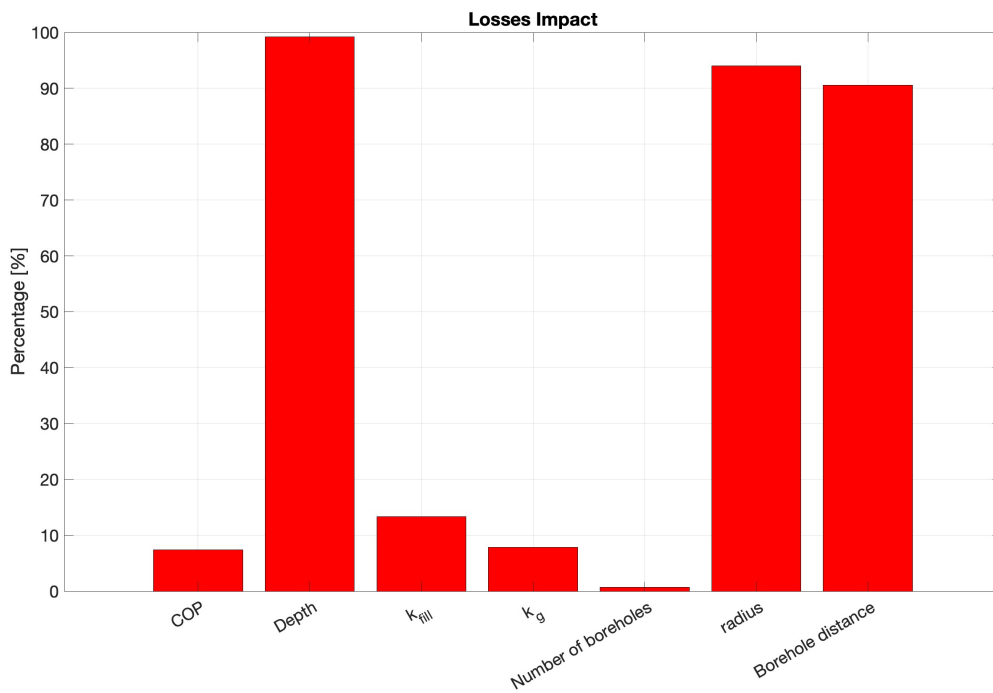
Once this analysis has been performed for the base case, heat losses are evaluated also for each storage parameter during the sensitivity analysis.

The aim of this calculation is to assess the storage parameters that cause the highest heat losses worsening the system performances.

Results for Load 1 and Load 2 are shown in figure 7.23 and they highlight that the BHEs depth, the radius and distance between the boreholes significantly affect system's performance.



(a) Load 1

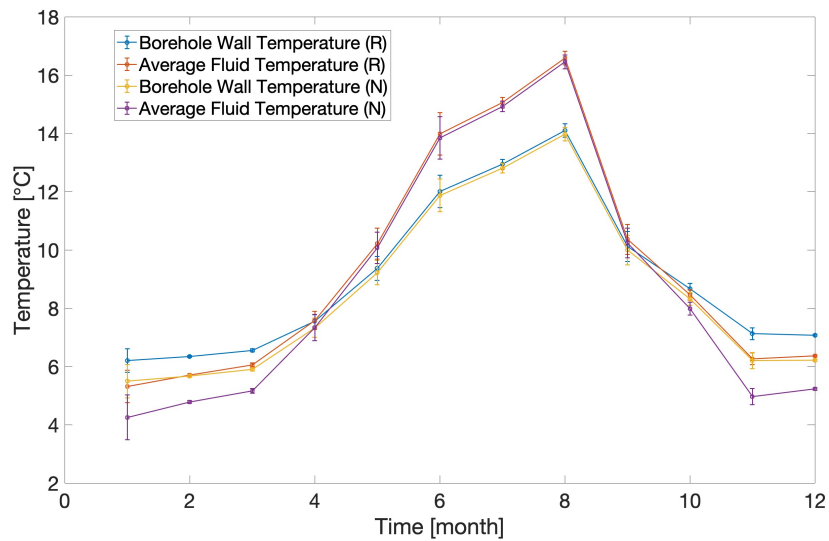


(b) Load 2

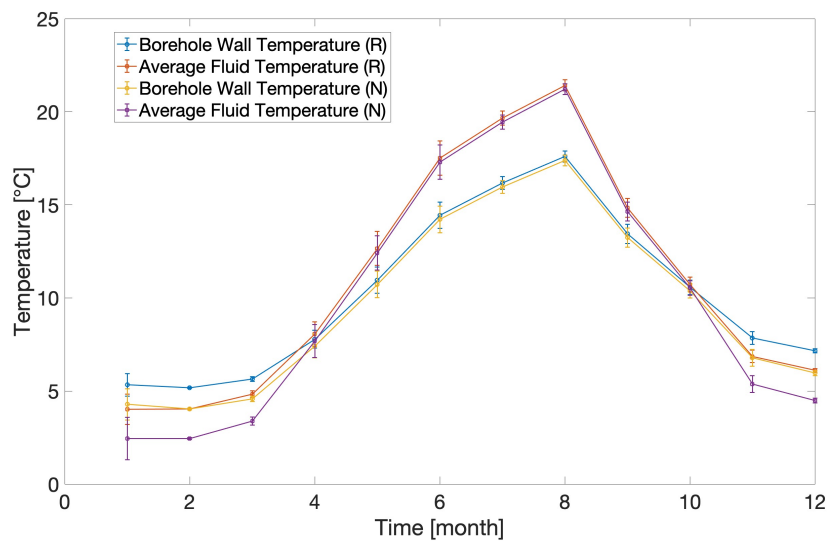
Figure 7.23: Losses analysis on different storage parameters

7.5 Effect of the HP's COP Model on the Temperatures' Profiles

In this section, the effect of the HP's COP model on the borehole wall temperature and average fluid temperature will be explained.



(a) Load 1



(b) Load 2

Figure 7.24: HP's COP model impact on temperature profiles

Results shown in figure 7.24 highlight slight variation of temperature levels passing from the regression model, identified with letter R, to the use of the COP function for the HP, identified with letter N.

Specifically, being the COP values higher with the new model the amount of energy extracted during the discharging season is higher.

Thus, the temperatures reached with the semi-dynamic model during winter are lower if compared to the ones obtained with the regression model.

Chapter 8

Future Work

System improvements are crucial for enhancing efficiency, effectiveness, reliability and performances of the overall storage system.

In this section, suggestions are provided for potential future work.

The goal of this master thesis was to gather knowledge regarding the main technical aspects of BTES, analyze the thermal behavior of the storage system through the implementation of the *Load Aggregation Algorithm* and evaluate the most critical storage parameters that highly affect the system performances. Information and data required have been acquired from specific papers and references.

Results from MATLAB simulations have been compared with literature study to verify their truthfulness.

Future works should be focused on the development of a dynamic and complete model of the heat pump. In fact, given a suitable value of water mass flow rate inside the BTES and knowing the amount of energy stored inside the storage it is possible to develop a dynamic heat pump model that is able to thermally couple the heat pump itself to the district heating network.

In particular, the aim of this point is to realize a model in which the HP's COP is adjusted according to the load from the DH network and not kept constant.

In accordance to the previous point, the necessity of developing a more complex storage system model is impelling. In particular, experimental and in-situ tests should be carried out to obtain results from simulations as reasonable as possible.

Techno-economic analysis and system optimization should be performed as well. Since the aim of this master thesis is restricted to the system design phase the results obtained are not viable in real power plant operations, specifically because the economic implications

of the compressor power and of the outlet temperature of the condenser are not taken into consideration.

If all the previous points are satisfied it is possible to obtain a dynamic model of the overall system and to have an idea of how the different parameters vary according to the DH loads.

Finally, according to the Statkraft Company target the heating of the boreholes during winter is highly suggested. In fact, charging the boreholes for a short period of time during winter, when the temperature is above 0 °C, may positively affect the system performance.

This scenario is feasible when electricity prices are low and BTES temperatures are higher to reduce heat losses.

Chapter 9

Conclusion

This chapter contains a summary of the main results obtained from the simulations and major improvements to be made to the system to obtain more realistic outcome.

Besides the investigation of the main theoretical aspects concerning BTES systems and their modeling procedure, the aim of this thesis is to compute a first design phase of such a system and to provide an idea of which are the parameters that mostly affect system performance both positively and negatively. Interesting results have been shown by performing the sensitivity analysis.

Additionally, the heat losses analysis and the variability of the HP's COP on the main temperature profiles have been carried out.

Finally, a long-term analysis has been computed to provide further information about the storage behavior.

The sensitivity analysis has shown that for both Load 1 and Load 2 the most critical storage parameters are the borehole depth and the distance between the BHEs. Particularly, by choosing a depth of 50 *m* and a distance of 2 *m* the storage capacity is altered, specifically the amount of energy injected or extracted is distributed over a smaller volume causing an increase in terms of heat losses.

As it is possible to deduce, it is highly desirable that these parameters will be included in the optimization phase of the system to find the suitable trade-off between the losses and the system efficiency.

From the heat losses analysis it has been possible to discover that if the values of the BHE's depth, radius and mutual distance are inappropriate the heat losses are extremely high. In particular, they are assessed to be between 88% and 98%.

In conclusion, other relevant results are related to the analysis of the long-term storage

behavior and to the effect of a variable COP on system performance.

Regarding the long-term storage behavior, results have shown that the global trend is strictly related to the amount of energy injected or extracted. Specifically, if the amount of energy extracted is higher than the amount of energy injected the global trend will be a decreasing trend and vice versa.

Regarding the effect of a variable COP on system performance, results demonstrate that being the storage not thermally coupled to the heat pump temperature profiles are slightly affected by the variation of the HP's COP.

Bibliography

- [1] Fredrik Schmidt. Large scale heat storage for district heating. Master’s thesis, NTNU, 2020.
- [2] Göran Hellström. *Ground heat storage: thermal analyses of duct storage systems*. Lund University, 1991.
- [3] Helge Skarphagen, David Banks, Bjørn S Frengstad, Harald Gether, et al. Design considerations for borehole thermal energy storage (btes): A review with emphasis on convective heat transfer. *Geofluids*, 2019, 2019.
- [4] Min Li and Alvin CK Lai. Review of analytical models for heat transfer by vertical ground heat exchangers (ghes): A perspective of time and space scales. *Applied Energy*, 151:178–191, 2015.
- [5] Johan Claesson and Saqib Javed. An analytical method to calculate borehole fluid temperatures for time-scales from minutes to decades. *ASHRAE Transactions*, 117(2), 2011.
- [6] Changxing Zhang, Yusheng Wang, Yufeng Liu, Xiangqiang Kong, and Qing Wang. Computational methods for ground thermal response of multiple borehole heat exchangers: A review. *Renewable Energy*, 127:461–473, 2018.
- [7] Vilde Eikeskog. Analyses and evaluation of the heat pump based energy supply system integrating short-and long term storages–analyses of sizing and operation. Master’s thesis, NTNU, 2020.
- [8] Sara Bordignon, Jeffrey D Spitler, and Angelo Zarrella. Simplified water-source heat pump models for predicting heat extraction and rejection. *Renewable Energy*, 220:119701, 2024.
- [9] Kauko H. Tereshchenko T. Nord N., Nielsen E. K. L. Challenges and potentials for low-temperature district heating implementation in norway. *Energy*, pages 889–902, 2018.

- [10] Rohde D. Hafner A. Nord N Kauko H., Kvalsвик K. H. Dynamic modelling of local low-temperature heating grids: A case study for norway. *Energy*, pages 289–297, 2017.
- [11] Fung A. S. Rad F. M. Solar community heating and cooling system with borehole thermal energy storage—review of systems. *Renewable and Sustainable Energy Reviews*, pages 1550–1561, 2016.
- [12] Rosen M. A. Dincer I. Thermal energy storage: systems and applications. *John Wiley Sons*, 2021.
- [13] Six D. Tant P. De Rybel T. Driesen J. Geth F., Tant J. Techno-economical and life expectancy modeling of battery energy storage systems. In *Proceedings of the 21st International Conference on Electricity Distribution (CIRED), Frankfurt, Germany*, pages 6–9, 2021.
- [14] Thomas Kohl, Renzo Brenni, and Walter Eugster. System performance of a deep borehole heat exchanger. *Geothermics*, 31(6):687–708, 2002.
- [15] Signhild EA Gehlin, PhD Jeffrey Spitler, and PE Göran Hellström. Deep boreholes for ground source heat pump systems—scandinavian experience and future prospects.
- [16] Tuğçe Başer, Ning Lu, and John S McCartney. Operational response of a soil-borehole thermal energy storage system. *Journal of Geotechnical and Geoenvironmental Engineering*, 142(4):04015097, 2016.
- [17] Arefeh Hesaraki, Sture Holmberg, and Fariborz Haghighat. Seasonal thermal energy storage with heat pumps and low temperatures in building projects—a comparative review. *Renewable and Sustainable Energy Reviews*, 43:1199–1213, 2015.
- [18] Ali H Tarrad. A perspective model for borehole thermal resistance prediction of a vertical u-tube in geothermal heat source. *Athens Journal of Technology and Engineering*, 7(2):73–92, 2020.
- [19] Yian Gu and Dennis L O’Neal. Development of an equivalent diameter expression for vertical u-tubes used in ground-coupled heat pumps. *Transactions-American Society of Heating Refrigerating and air Conditioning Engineers*, 104:347–355, 1998.
- [20] Malin Malmberg, Willem Mazzotti, José Acuña, Henrik Lindstahl, and Alberto Lazarotto. High temperature borehole thermal energy storage—a case study. 2018.
- [21] M Reuss. The use of borehole thermal energy storage (btes) systems. In *Advances in thermal energy storage systems*, pages 117–147. Elsevier, 2015.

- [22] Heyi Zeng, Nairen Diao, and Zhaohong Fang. Heat transfer analysis of boreholes in vertical ground heat exchangers. *International journal of heat and mass transfer*, 46(23):4467–4481, 2003.
- [23] Saqib Javed and Jeffrey D Spitler. Calculation of borehole thermal resistance. In *Advances in ground-source heat pump systems*, pages 63–95. Elsevier, 2016.
- [24] Cenk Yavuzturk and Jeffrey D Spitler. A short time step response factor model for vertical ground loop heat exchangers. *ASHRAE transactions*, 105(2):475–485, 1999.
- [25] Heyi Y Zeng, Nairen R Diao, and Zhaohong H Fang. A finite line-source model for boreholes in geothermal heat exchangers. *Heat Transfer—Asian Research: Co-sponsored by the Society of Chemical Engineers of Japan and the Heat Transfer Division of ASME*, 31(7):558–567, 2002.
- [26] Leonard R Ingersoll, Otto J Zobel, and Alfred Cajori Ingersoll. Heat conduction with engineering, geological, and other applications. (*No Title*), 1954.
- [27] Min Li and Alvin CK Lai. New temperature response functions (g functions) for pile and borehole ground heat exchangers based on composite-medium line-source theory. *Energy*, 38(1):255–263, 2012.
- [28] Johan Claesson and Per Eskilson. Conductive heat extraction to a deep borehole: Thermal analyses and dimensioning rules. *Energy*, 13(6):509–527, 1988.
- [29] Massimo Cimmino and Michel Bernier. A semi-analytical method to generate g-functions for geothermal bore fields. *International Journal of Heat and Mass Transfer*, 70:641–650, 2014.
- [30] Mostafa H Sharqawy, Esmail M Mokheimer, and Hassan M Badr. Effective pipe-to-borehole thermal resistance for vertical ground heat exchangers. *Geothermics*, 38(2):271–277, 2009.
- [31] Min Li and Alvin CK Lai. Thermodynamic optimization of ground heat exchangers with single u-tube by entropy generation minimization method. *Energy Conversion and Management*, 65:133–139, 2013.
- [32] HS Carslaw and JC Jaeger. *Conduction of heat in solids.* (clarendon press, oxford.). 1959.
- [33] JD Deerman. Simulation of vertical u-tube ground-coupled heat pump systems using the cylindrical heat source solution. *ASHRAE Transaction*, 3472:287–295, 1990.
- [34] C Yavuzturk, AD Chiasson, and JE Nydahl. Simulation model for ground loop heat exchangers. *Ashrae Transactions*, 115(2), 2009.

- [35] Ali Salim Shirazi and Michel Bernier. Thermal capacity effects in borehole ground heat exchangers. *Energy and Buildings*, 67:352–364, 2013.
- [36] Min Li and Alvin CK Lai. Analytical model for short-time responses of ground heat exchangers with u-shaped tubes: Model development and validation. *Applied energy*, 104:510–516, 2013.
- [37] Min Li, Ping Li, Vincent Chan, and Alvin CK Lai. Full-scale temperature response function (g-function) for heat transfer by borehole ground heat exchangers (ghes) from sub-hour to decades. *Applied Energy*, 136:197–205, 2014.
- [38] Patricia Monzó, Jose Acuna, Palne Mogensen, and Björn Palm. A study of the thermal response of a borehole field in winter and summer. In *International conference on applied energy ICAE. Jul*, pages 1–4, 2013.
- [39] Marco Fossa, Stefano Morchio, Antonella Priarone, and Samuele Memme. Accurate design of bhe fields for geothermal heat pump systems: The ashrae-tp8 method compared to non aggregated schemes applied to different european test cases. *Energy and Buildings*, 303:113814, 2024.
- [40] Hans-Jörg G Diersch and Dan Bauer. Analysis, modeling, and simulation of underground thermal energy storage systems. In *Advances in Thermal Energy Storage Systems*, pages 173–203. Elsevier, 2021.
- [41] Huaajun Wang, Yahui Cui, and Chengying Qi. Effects of sand–bentonite backfill materials on the thermal performance of borehole heat exchangers. *Heat transfer engineering*, 34(1):37–44, 2013.
- [42] Michael Jokiel, Daniel Rohde, Hanne Kauko, and Harald Taxt Walnum. Integration of a high-temperature borehole thermal energy storage in a local heating grid for a neighborhood. In *International Conference Organised by IBPSA-Nordic, 13th–14th October 2020, OsloMet. BuildSIM-Nordic 2020. Selected papers*. SINTEF Academic Press, 2020.
- [43] Raphaël Croteau and Louis Gosselin. Correlations for cost of ground-source heat pumps and for the effect of temperature on their performance. *International journal of energy research*, 39(3):433–438, 2015.

Ringraziamenti

Vorrei riservare questa sezione per ringraziare tutti coloro i quali hanno reso speciale questo viaggio. A tutti gli effetti il mio traguardo è anche un vostro traguardo.

In particolare, ringrazio il Professore Vittorio VERDA e la Professoressa Elisa GUELPA per aver creduto in me sin dall'inizio offrendomi la possibilità di svolgere la tesi in un contesto internazionale quale la NTNU e per il grande supporto tecnico e umano durante lo svolgimento della tesi.

I would like to thank my supervisor Professor Natasa NORD and her research team for endless help, knowledge and support through every step of this project.

Ringrazio infinitamente la mia famiglia per avermi sostenuta e aver creduto in me anche quando nemmeno io ci ho creduto.

Mi avete insegnato che grazie all'impegno anche gli ostacoli più ardui possono essere superati, che il bicchiere non è sempre del tutto vuoto ma che dagli errori e dalle sfide è sempre possibile trarre insegnamenti e che i fallimenti rappresentano, in realtà, nuovi inizi e rinascite individuali.

So che non deve essere stato semplice per voi starmi vicina in questi cinque anni ma lo avete fatto nel miglior modo possibile e sicuramente non bastano queste poche righe per esprimere tutta la gratitudine e la stima che nutro nei vostri confronti.

Ho cercato di rendervi fieri di me e spero di esserci riuscita con il raggiungimento di questo traguardo.

Ringrazio Gerardo perché sin da subito hai saputo capirmi e indicarmi la strada giusta con grande senso del dovere. Ti ringrazio per le parole di stima che hai espresso nei miei confronti in svariate occasioni e spero di esserne all'altezza.

Senza di te non ce l'avrei mai fatta.

Ringrazio Marcello, Gaetano, Bachisio, Madalina, Gas, Lollo e Pasquale anche se vi conosco da poco siete stati il mio primo vero gruppo di amici e per questo avrete sempre un posto importante nel mio cuore. Siete davvero delle persone speciali e ognuno di voi è

stato illuminante.

Siete e siete stati presenti per me nei momenti più belli, con la vostra innata simpatia e contagiante voglia di vivere, ma anche in quelli più difficili supportandomi e ascoltando i miei lunghissimi e ripetitivi discorsi.

Avete alleggerito le sessioni più lunghe, gioito con me per i bei traguardi raggiunti e mi avete affiancato nelle sconfitte temporanee senza mai stancarvi di me. Per tutto questo vi sarò sempre grata.

Ringrazio Ilaria per avermi accompagnata passo dopo passo in questa esperienza.

Grazie per tutte le videochiamate notturne e il supporto morale che mi hai dato.

Sei stata sempre sincera e non hai mai preteso niente in cambio per tutto l'aiuto disinteressato che mi hai donato.

Ringrazio Corinna per aver condiviso con me la parte più piccola ma più significativa di questo tragitto.

Abbiamo pianto, sofferto e gioito insieme. Ci siamo ascoltate, confrontate e confidate.

Grazie per essere stata così tanto in così poco tempo, hai reso questo viaggio molto più leggero e divertente.

Ringrazio Sofia per il suo costante supporto e la sua amicizia.

Mi hai sostenuto, incoraggiato e spronato. Hai condiviso con me momenti di gioia e di sfide, e insieme abbiamo superato ogni tipo di ostacolo.

Le risate, le conversazioni e le avventure con te sono state preziose aggiunte alla mia esperienza universitaria.

Grazie per essere sempre al mio fianco, per ascoltare le mie lamentele, per darmi consigli saggi e per aver condiviso con me le gioie di questi anni.

Ringrazio Tommaso per essere stato presente sin da subito.

Mi hai insegnato a guardare la vita con occhi diversi e sei sempre stato al mio fianco anche quando facevo di tutto per tenerti lontano.

Abbiamo condiviso insieme questa esperienza e siamo stati l'uno la spalla dell'altro spronandoci e sostenendoci a vicenda.

Grazie per avermi sempre valorizzata e avermi incluso nelle decisioni più importanti che hai dovuto prendere.

Grazie per avermi insegnato ad affrontare le paure a testa alta e a superare tutte le 'montagne' che sembravano insormontabili.

Grazie per essermi stato accanto nonostante la lontananza e le difficoltà quotidiane che abbiamo dovuto affrontare: sei e sei stato un punto di riferimento importante.

Ringrazio il mio coinquilino Giovanni: all'inizio abbiamo avuto qualche incomprensione e non siamo stati in grado di comprendere l'uno il valore dell'altro.

Siamo cresciuti insieme e grazie al rapporto che si è creato siamo diventati l'uno la spalla dell'altro.

So che posso contare su di te e per me sei stato significativo.

Ringrazio i miei amici conosciuti a Trondheim, in particolare, Aurora e Francesco.

Sono contenta di aver condiviso con voi questi sei mesi in cui abbiamo completamente stravolto le nostre vite adattandoci a situazioni complesse e temperature inusuali.

Grazie a voi ho affrontato i sei mesi più intensi della mia vita in maniera inaspettatamente leggera.

Ringrazio Greta per essere stata il mio principale punto di riferimento.

Grazie per la tua gentilezza e per l'infinito affetto che continui a donarmi senza mai stancarmi di me.

Sei davvero preziosa.

Vorrei ringraziare tutti i compagni di corso e le persone con cui ho condiviso questi anni meravigliosi ma intensi.

In parte i miei traguardi sono legati a voi: mi avete insegnato che tutto è possibile e che il confronto è fondamentale.

Ho trovato in voi il giusto stimolo, la giusta motivazione per tendere sempre all'eccellenza e spingermi oltre la comfort zone.

Infine, vorrei ringraziare me stessa per essere riuscita ad arrivare fin qui.

Sono state molteplici le volte in cui ho pensato che mollare sarebbe stato più semplice che continuare, ma mi sbagliavo.

In questi cinque anni mi sono spesso chiesta se fossi all'altezza del percorso intrapreso e spesso ho pensato che non fossi abbastanza brava.

Con il tempo ho realizzato che sfide impossibili non ne esistono, al contrario ci sono quelle più semplici e quelle più difficili e sono soprattutto queste ultime che ci aiutano a crescere e a diventare le persone che siamo.